DE GRUYTER

Rev Chem Eng 2025; aop

Review

Karan Sharma, Manishkumar D. Yadav, Abhishek Sharma, Subhankar Bhandari, Srikumar Ghorui and Jyeshtharaj B. Joshi*

Engineering insights into thermal plasma processing for plastic waste management: a review

https://doi.org/10.1515/revce-2025-0012
Received March 5, 2025; accepted August 19, 2025;

Abstract: The rapid accumulation of plastic waste due to its non-biodegradability and increasing global consumption presents a significant environmental challenge. Conventional thermochemical waste management techniques, such as pyrolysis and gasification, offer partial solutions but suffer from secondary pollutant formation, inefficiencies, and scalability issues. Thermal plasma-assisted processes, operating at extreme temperatures of 1,500–5,000 °C, present a promising alternative by leveraging high-energy plasma arcs to achieve complete waste destruction, converting plastic into syngas and inert slag while minimizing hazardous by-products like dioxins and tars. Despite being studied over decades, the commercialization of plasma technologies remains limited due to high capital costs, proprietary technology barriers, and suboptimal reactor designs. The scalability of these systems depends on optimizing energy efficiency and feedstock adaptability, which can be addressed through advanced reactor design. This review systematically evaluates thermal plasma technology for plastic waste treatment through chemical engineering analysis of plasma-specific reaction kinetics under rapid heating conditions, coupled heat/mass modelling in high-temperature reactors, and computational optimization of torch configurations and reactor geometries. Key knowledge gaps are analyzed, including electrode erosion dynamics, plasma gas selection trade-offs, unaddressed radiation effects, and lack of thermal plasma-specific kinetic-modelling and experimentation, while presenting strategies to overcome these limitations through both modeling and experimental approaches.

Keywords: plasma processing; plastic waste; solid waste management; plasma reactor design; kinetics; scale-up

1 Introduction

Plastic waste, due to its non-degradable nature, versatility, and widespread use, has emerged as a critical component of several complex and difficult waste streams. It is not just present in household and municipal solid waste (MSW), but also constitutes a significant fraction of other challenging streams such as agricultural waste (e.g., mulch films, pesticide containers), electronic waste (plastic housings, circuit board substrates), refuse-derived fuel (RDF), medical waste (syringes, tubing, IV bags), automotive shredder residue, multilayer packaging (MLPs), and even construction and demolition debris (e.g., insulation foams, PVC pipes). These streams are often heterogeneous, contaminated, and non-segregated, making plastic waste management challenging (Buekens and Zhou 2014; Guo et al. 2024; Joseph et al. 2021; Mtibe et al. 2023; Vox et al. 2016). The accumulation of end-of-life plastic in landfills and marine bodies accompanied by the so-called mismanaged “plastic emissions” led to 193.12 MMT of GHG emissions in 2019. In the same year plastic waste accounted for 3.3 % of the global CO_2 emissions (Cottom et al. 2024; Our World in Data 2024). The situation worsened during the COVID-19 pandemic, which spurred increased plastic consumption (Choudhury et al. 2022). This combined with excessive fossil-fuel usage, has intensified

---

***Corresponding author: Jyeshtharaj B. Joshi**, Department of Chemical Engineering, Institute of Chemical Technology, N. P. Marg, Matunga (E), Mumbai, 400019, India, E-mail: jbjoshi@gmail.com. https://orcid.org/0000-0002-4945-0788

Karan Sharma, Department of Chemical Engineering, Institute of Chemical Technology, N. P. Marg, Matunga (E), Mumbai, 400019, India; and J.B. Joshi Research Foundation, Mumbai, India

Manishkumar D. Yadav, Department of Chemical Engineering, Institute of Chemical Technology, N. P. Marg, Matunga (E), Mumbai, 400019, India

Abhishek Sharma, Department of Biotechnology & Chemical Engineering, Manipal University Jaipur, Dehmikalan, Jaipur, Rajasthan, 303007, India; and Department of Chemical Engineering, Birla Institute of Technology and Science, Pilani K K Birla Goa Campus, Goa, India

Subhankar Bhandari and Srikumar Ghorui, Laser & Plasma Technology Division, Bhabha Atomic Research Centre, Mumbai, 400085, India

the global environmental crisis (MacLeod et al. 2021). While the UN initiatives ban single-use plastics (UNEP – UN Environment Programme 2024) and businesses adopt plastic credit systems (Lee 2021), plastics remain vital to modern life. This paradox highlights the urgent need for effective plastic waste management strategies.

Thermo-chemical upcycling techniques like pyrolysis (Dai et al. 2022), gasification (Lopez et al. 2018), and solvolysis (Abedsoltan 2023) for mixed plastic wastes have garnered significant interest from industrialists for their potential to produce fuels and chemicals from plastic waste. The plastic to fuel industry was valued at $ 531.1 M in 2023, mostly dominated by pyrolysis worldwide and is projected to grow at CAGR of 26.1 % between 2024 and 2030 (Grand View Research 2024). Despite the huge spike in interest, these techniques do face operational limitations in mitigating plastic pollution effectively. Operational challenges like variable waste composition, sticky behavior of plastics, reliance on catalysts, risks of catalyst poisoning, formation and handling of corrosive tar, inconsistency in product quality, and slower conversion rates (Dogu et al. 2021; Lopez et al. 2018; Qureshi et al. 2020). Moreover, despite the controlled oxygen supply, the formation of dioxins and furans are difficult to be mitigated due to the presence of chlorinated impurities, improper reactor designs leading to larger and often uncontrolled residence times, a temperature range of 300–800 °C in conventional pyrolysis, and slow cooling rates which is suitable for the formation of these carcinogenic pollutants (Bei et al. 2022; Safavi et al. 2021, 2022; Tang et al. 2024; Zhang et al. 2018). On the other hand, plasma processing is one such thermo-chemical conversion technique for waste, which, if appropriately designed by addressing its unique operational considerations, can overcome such issues.

Plasma processing has emerged as a promising technology for solid and hazardous waste management. Since its discovery in 1879 by Sir William Crookes, plasma, originally referred to as “radiant matter”, has evolved significantly in its applications as can be seen in Figure 1. The term “plasma” was coined by Irwing Langmuir in 1928, marking the beginning of plasma physics, which paved the way for its industrial applications (Sikarwar et al. 2020; Tonks and Langmuir 1929). The technology gained traction in the late 1930s with the implementation of the first non-transferred plasma torches for the production of acetylene. By the 1980s, thermal plasma processes were being piloted for industrial toxic waste reduction and material science applications. The 1990s saw the establishment of commercial plants utilizing thermal plasma for treating hazardous waste, highlighting its versatility in industrial applications. Today, plasma technology is recognized for its potential in waste-to-energy processes and being integrated into circular economy models and waste management strategies (Ramos et al. 2019a,b). Thermal plasma processing techniques like plasma – pyrolysis, gasification, reforming, melting, and vitrification have been proven to be suitable for a wide variety of waste applications comprising of plastic wastes (Guo and Kim 2010; Punčochář et al. 2012; Rida Galaly et al. 2024), municipal solid wastes (MSW) (Mazzoni and Janajreh 2017; Nemmour et al. 2023; Tavares et al. 2019), biomedical waste (Amirahmadi et al. 2024; Li et al. 2024; Paulino et al. 2020, 2022), biomass (Hlina et al. 2014; Ma et al. 2020, 2020; Sikarwar et al. 2022b), inorganic waste (Cerqueira et al. 2006; Li et al. 2023; Ma et al. 2021), hazardous (Cvetinović et al. 2024; Ma et al. 2023; Okati et al. 2021; Sanito et al. 2022; Sikarwar et al. 2021, 2024; Zhovtyansky and Valinčius 2018), and radioactive wastes (Benedetto et al. 2024; Gonçalves et al. 2022; Ma et al. 2024) as clearly illustrated in Supplementary Figure S1. Thermal plasma processing heats the feed directly through electrically powered high-temperature plasma arcs (1,500 °C to 5,000 °C), enabling rapid heating rates and high energy efficiency compared to conventional systems relying on indirect heating, such as external gas-fired heaters or resistive elements (Agun et al. 2022; Ofori-Boateng 2024). This reduces the time constant to achieve desired temperatures, allowing for shorter residence times and compact reactors, thereby supporting process intensification (Stankiewicz 2020). Additionally, thermal plasma processing accelerates reaction rates due to the presence of high-energy charged species (ions, electrons, radicals) energized by a strong electric field, enabling faster kinetics and enhanced gas-phase reactivity compared to conventional catalytic processes (Ganza and Lee 2023). Another advantage of plasma processing is its ability to safely treat chlorine-containing mixed plastic waste streams, the high temperatures and reducing conditions facilitate volatilization of chlorine as HCl, minimizing the risk of formation of persistent organic pollutants (Chu et al. 2023). In traditional methods like incineration or gasification, lower temperatures often result in the formation of hazardous carcinogens, such as polychlorinated dibenzodioxins (PCDDs) and dibenzofurans (PCDFs). These compounds form when chlorine reacts with organic materials under suboptimal conditions. However, plasma’s extremely high energy density and temperature fully dissociate these harmful compounds, ensuring safer handling of plastic waste (Ganza and Lee 2023; Rida Galaly et al. 2024; Yousef et al. 2024). Additionally, thermal plasma systems, when integrated with appropriate gas-cleaning units, similar to traditional thermochemical processes can effectively reduce secondary pollutant emissions, ensuring regulatory standards are met. However, the conversion and reaction behavior of plastic waste are not merely functions

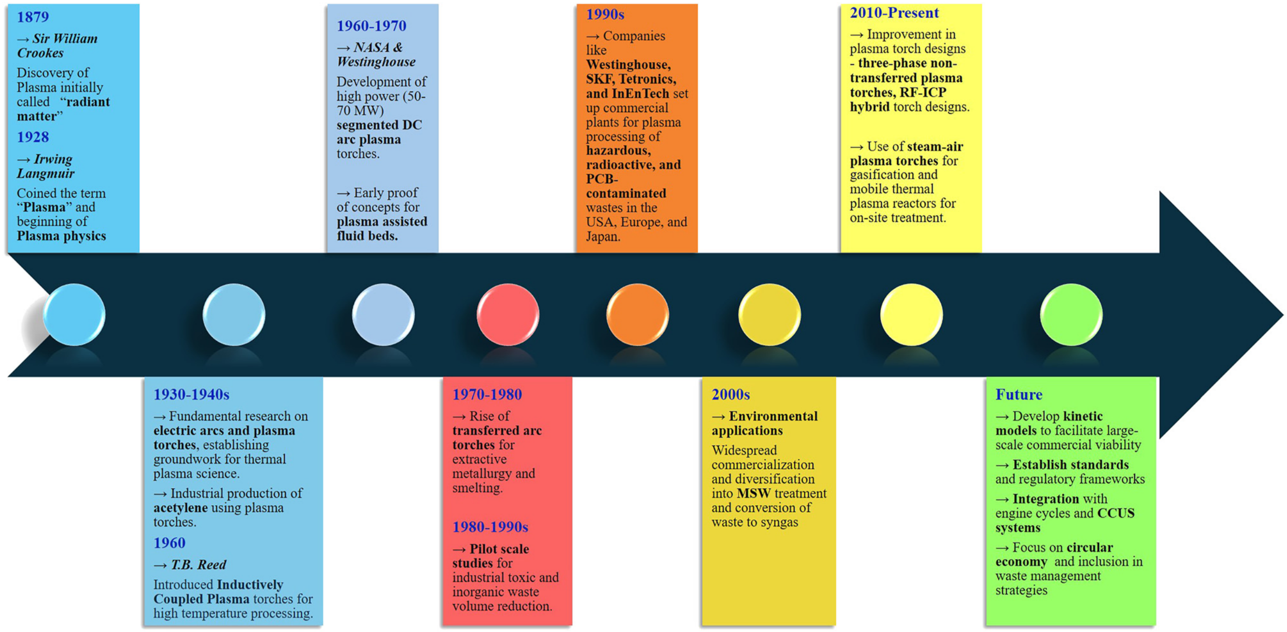

Figure 1: Evolution of thermal plasma technology for waste processing.

of temperature and waste composition but also rely significantly on the reactor design which is influenced by reaction kinetics, residence time, and heat and mass transfer inside the reactor (Janajreh et al. 2021). In order to feasibly scale-up the thermal plasma processing technologies aforementioned factors must be critically investigated and discussed.

Table 1 summarizes several recently published reviews that have successfully provided an overview of thermal plasma processing techniques, and assessed – the effects of varying parameters, multiple feedstock combinations, energy and economic efficiency of the process, and environmental impacts. Their key focuses and future suggestions are outlined in Supplementary Table S1. Despite this extensive body of work, a fundamental engineering understanding – essential for the successful scale-up of plasma technology for plastic waste treatment – remains scarce in such published reviews. Critical research gaps persists including, unexplored reaction kinetics under thermal plasma-specific conditions, limited studies on material flow and residence time distribution, techno-economic analysis often extrapolated from conventional thermochemical systems, and fewer experiments with real-waste. The current review aims at addressing these gaps from a chemical engineering perspective. The succeeding chapters are structured as follows: Chapter 2 reviews plasma pyrolysis/gasification studies for plastic waste; Chapter 3 compares plasma torch designs and their operational implications; Chapter 4 analyzes feedstock-property-parameter interplay, including plasma gas selection for scalability; Chapter 5 examines thermal plasma-specific heat/mass transfer, degradation kinetics, and CFD-based flow/temperature profiles; Chapter 6 proposes a scaling methodology grounded in chemical engineering fundamentals; Chapter 7 evaluates techno-economic feasibility and commercialization drivers; Chapter 8 documents past/present commercialization attempts and key lessons. By integrating these aspects, this study aims to bridge the gap between laboratory-scale research and industrial deployment of plasma-based plastic waste treatment.

2 Plasma processing techniques

Thermo-chemical conversion processes vary primarily by oxygen content and temperature. Unlike combustion (excess oxygen), pyrolysis and gasification use sub-stoichiometric oxygen, reducing harmful pollutant formation (Shah et al. 2023). This makes them environmentally preferable for plastic waste treatment. Given plastics' hydrocarbon nature and the potential for diverse product outputs, thermal plasma technology has emerged as a promising approach, with process selection ultimately depending on desired products.

2.1 Plasma pyrolysis

During the pyrolysis of plastic, the material undergoes a series of thermal and chemical degradation steps, breaking

Table 1: Overview of recent published reviews on thermal plasma processing of wastes.

Review title	Key focus	Future studies suggested	Year	References
A review of recent advancement in plasma gasification: a promising solution for waste management and energy production	1, 3	C, F, I	2024	Nagar and Kaushal (2024)
A review on plasma gasification of solid residues: recent advances and developments	1, 3, 7	A, B	2022	Oliveira et al. (2022)
A critical review on solid waste management using plasma pyrolysis technology	2, 5	A, B, D	2022	Bhatt et al. (2022)
A review on converting plastic wastes into clean hydrogen via gasification for better sustainability	1, 4, 10	G, H	2022	Midilli et al. (2022)
Life cycle thinking of plasma gasification as a waste-to-energy tool: review on environmental, economic and social aspects	6, 7	I, J	2022	Ramos and Rouboa (2022)
A comprehensive review of the application of plasma gasification technology in circumventing the medical waste in a post COVID-19 scenario	1, 7, 9a	C, E, I	2022	Kaushal et al. (2024)
An overview of the technological applicability of plasma gasification process	6, 8	I, J	2020	Achinas (2019)
Thermal plasma treatment of medical waste	1, 2, 7, 8, 9a	D, E, H	2020	Cai and Du (2021)
PCDD/PCDFs: a burden from hospital waste disposal plant; plasma arc gasification is the ultimate solution for its mitigation	6, 7, 9a	I, J	2020	Das et al. (2020)
A comprehensive review on advanced thermochemical processes for bio-hydrogen production via microwave and plasma technologies	1, 2, 4, 9c	A, B, C	2020	Inayat et al. (2023)
Progress in waste utilization via thermal plasma	1,2,3,8,9d	A, B, F, H	2020	Sikarwar et al. (2020)
Plasma gasification of municipal solid waste for waste-to-value processing	1, 7	A, B, F, H	2019	Munir et al. (2019)

The legends for key focus and future studies are explained in Supplementary Table S1.

down into simpler chemical species such as H_2, C, or their compounds, depending on the operating conditions. Typically, homolytic cleavage initiates the process, forming free radicals that propagate further degradation. In halogenated plastics like PVC, heterolytic cleavage occurs, producing HCl via dehydrochlorination (Zhang et al. 2022). These radicals undergo secondary reactions such as β-scission, hydrogen abstraction, and radical recombination, with product distribution influenced by temperature, heating rate, and residence time (Gracida-Alvarez et al. 2018). The pyrolysis reaction mechanism, using polypropylene as an illustrative example, is described in Equations (1)–(6).

$$\begin{aligned} &-\mathrm{CH_2}-\mathrm{CH(CH_3)}-\mathrm{CH_2}-\mathrm{CH(CH_3)}-\underset{\rightarrow}{\underline{\Delta}}-\mathrm{CH_2}\\ &-\mathrm{CH^*(CH_3)}+\mathrm{CH_2^*}-\mathrm{CH(CH_3)}- \end{aligned} \tag{1}$$

$$\begin{aligned} -\mathrm{CH_2}-\mathrm{CH^*(CH_3)} \ \rightarrow\ &\mathrm{CH_2}=\mathrm{CH(CH_3)}+\mathrm{CH_2^*}\\ &-[\beta-\mathrm{scission}] \end{aligned} \tag{2}$$

$$\begin{aligned} -\mathrm{CH_2^*}+\mathrm{CH_3^*} \ \rightarrow &\mathrm{CH_2}=\mathrm{CH(CH_3)}+\mathrm{CH_3}\\ &-\mathrm{CH_3}\ [\text{radical termination}] \end{aligned} \tag{3}$$

$$\mathrm{CH_2^*}-\mathrm{CH_3}\rightarrow\mathrm{CH_2}=\mathrm{CH_2}+\mathrm{H^*}\quad[\beta-\mathrm{scission}] \tag{4}$$

$$\begin{aligned} &2\mathrm{H^*}\\ &\rightarrow\mathrm{H_2}\ [\text{radical recombination and dehydrogenation}] \end{aligned} \tag{5}$$

$$\begin{aligned} \mathrm{CH_2}=\mathrm{CH(CH_3)}+\mathrm{H_2}\ \rightarrow &\mathrm{CH_3}-\mathrm{CH_2}\\ &-\mathrm{CH_3}\ [\text{hydrogenation}] \end{aligned} \tag{6}$$

Pyrolysis is classified into slow, fast, and flash processes based on the heating rate and residence time, with each focusing on producing either solid, liquid or gaseous products. Pyrolysis often produces complex product mixtures with limited value, typically used as furnace oil or boiler fuel. Catalytic pyrolysis using zeolites improves product selectivity by controlling residence time and secondary reactions, but mixed plastic feedstocks pose challenges like varied decomposition kinetics, catalyst coking, and PAH formation (Qureshi et al. 2020). In contrast, plasma pyrolysis better handles feedstock inconsistency, offering improved process stability.

Thermal plasma pyrolysis process utilizes plasma-generated heat to break down plastic waste into gas and solid products. This occurs at high temperatures, typically between 700 and 900 °C. A typical plasma pyrolysis setup, as illustrated in Figure 2, involves introducing shredded plastic waste into the reactor via a hopper or screw feeder. Once inside, the waste particles are subjected to rapid heating rates, around 10^6 K/s, powered by an AC or a DC arc plasma torch (Tang et al. 2003). The heated particles vaporize and exit into a cyclone, separating entrained solids, followed by gas cleaning in an alkali scrubber and bag filter. The resulting gas is either purified or released through a flame tower chimney. Plasma pyrolysis operates at lower temperatures compared to other plasma processes, providing the possibility to produce gas, liquid, and solid products. Various research studies highlight the process's potential are summarized in Table 2, which can broadly be categorized into three primary focuses: syngas and energy recovery, monomer and intermediate chemical recovery, and the production of solid carbonaceous materials.

Tang et al. (2003), investigated the plasma pyrolysis of polypropylene (PP) in a DC arc N_2 plasma reactor and reported consistently higher conversion efficiencies compared to thermal pyrolysis and catalytic pyrolysis across all feed rates. Punčochář et al. (2012), conducted a techno-economic assessment of a 1 TPD plastic waste plasma pyrolysis system, estimating energy recovery of 2.4 kW_e/kg of plastic converted. Bhatt et al. (2024) explored the pyrolysis of PET, PP, LDPE, and HDPE using a graphite electrode arc plasma. They observed that HDPE yielded the highest cold gas efficiency (66.12 %) due to greater H_2 and C_2H_2 production at 1,000 °C, while PET generated more CO (42 mol %), leading to a lower H_2/CO ratio. Further, Zhang et al. (2018), reported similar findings for PET pyrolysis in DC arc H_2 plasma. Several studies have demonstrated that plasma pyrolysis can selectively recover olefins and monomers under specific conditions. Guddeti et al. (2000a), used an RF-induced Ar plasma to depolymerize PE into a gas mixture rich in C_2–C_4 olefins, primarily ethylene and propylene. The forming gas flow rate inversely influenced propylene content by altering plasma temperature. In follow-up experiments, it was observed that higher plate power expanded the plasma jet volume, increasing residence time and thus enhancing propylene yield (Guddeti et al. 2000b). Zhang et al. (2017), applied a rotating DC arc H_2 plasma for pyrolysis of PE and PP, achieving peak plastic-to-gas conversion and acetylene selectivity of 95 % and 77.43 %, respectively. However, both declined beyond optimal input power due to excessive dilution of plasma energy. Plasma pyrolysis also allows for the production of valuable solid carbonaceous materials. Guo and Kim (2010), designed a graphite-lined double-chambered reactor to produce ultrafine carbon black from PS and HDPE. Carbon black yield increased with temperature (500–900 °C), and BET surface areas of 142.5 and 141.3 m^2/g were obtained for PS and HDPE, respectively. Fazekas et al. (2016) used RF-induced $Ar/H_2/O_2$ plasma to treat PVC, producing approximately 40 wt% soot and a gas rich in CO, CO_2, HCl, and C_2H_2. Toluene-extracted soot contained chlorinated PAHs, and higher O_2 content suppressed PAHs while increasing polychlorinated derivatives.

These studies underline the versatility of plasma pyrolysis in tailoring product outputs by controlling process parameters and feedstock. Though promising for single polymers, mixed plastic waste remains challenging due to poor selectivity and purity. Future work should optimize reactor design and plasma conditions to enhance scalability.

2.2 Plasma gasification

Gasification is the process of converting hydrocarbonaceous liquid or solid materials into gaseous products through substoichiometric oxidation at high temperatures ranging from 900 to 1,200 °C. This technology is increasingly recognized as a sustainable method for managing solid waste (Al-Ghouti et al. 2021; Mukherjee et al. 2020). The limited availability of oxygen in the process prevents the formation of harmful oxygen-derived pollutants such as NO_x and SO_x.

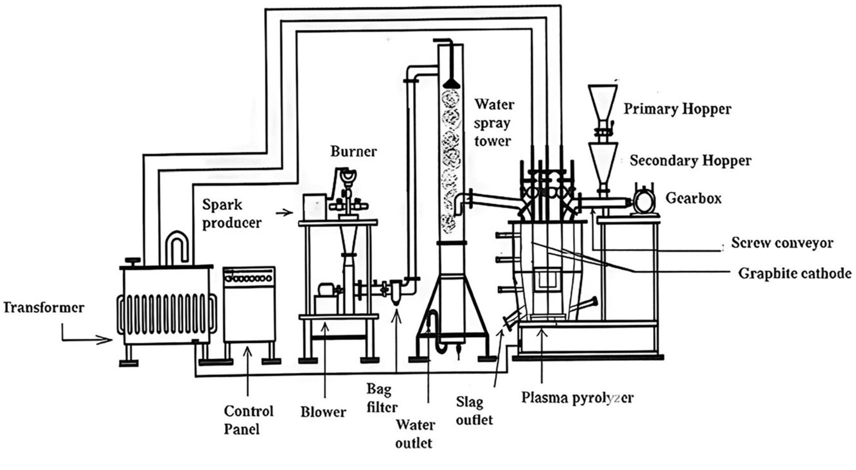

Figure 2: Schematic of plasma pyrolysis process. Reproduced with permission from ref. (Punčochář et al. 2012). Copyright 2012, Elsevier.

Table 2: Summary of studies on plastic waste treatment through plasma pyrolysis.

Feed	Particle size	Feed rate (g/min)	Forming gas	Plasma specs	Operating conditions	Output	References
PP	177–595 µm	60	N_2 – 83 slpm; 4 bar	DC arc – 26.4–62 kW 220–250 V 120–150 A	35.2 kW; carrier N_2 – 2 m^3/h; 1 bar	Gas – H_2, CO, C_2H_2, light HCs	Tang et al. (2003)
MPW	–	333	–	3× graphite electrode (φ –34 mm × 1,500 mm) Carbon electrode 400 mm × 120 mm × 50 mm	1,200 °C; 1 bar	Gas – H_2, CO, light HCs Slag	Punčochář et al. (2012)
LDPE	–	Batch	N_2	DC arc 270 W	625–860 °C; R.T. – 30 min; 7.8 °C/min; −0.95 bar	Oil – C_{10}–C_{28} (56.9 wt%)	Gabbar et al. (2017)
HDPE	–	Batch – 30 g	N_2 – 25 slpm	DC arc – 20 kW	900 °C; 1 bar	Gas – 5 wt% Liquid – 75 wt% Solid – 20 wt%	Guo and Kim (2010)
PS					800 °C; 1 bar	Styrene – 80 wt% BTX – 10 wt%	
PVC	150 µm	0.8–2.5	Ar – 15.5–35.5 slpm	RF induced – 15–25 kW	–	Gas – HCl, CO, CO_2, C_2H_2; solid-soot (20–40 wt%)	Fazekas et al. (2016)
PP	φ –50 × 120 mm	Batch	Ar – 18 slpm	DC arc 80–120 A	–	Carbon nano structures	Mohsenian et al. (2018)
PVC PE ABS PP	φ –50 × 120 mm	Batch	Ar – 18 slpm	DC arc 80–140 A	140 A	Gas – H_2, light HCs Carbon nano-spheres	Mohsenian et al. (2016)
PET	1–10 cm	166	–	Graphite electrode – 30 kW 100 V 300 A	900 °C; 1 bar	Gas – 79.7 wt% Solid – 15.5 wt%	Bhatt et al. (2024)
PP		83				Gas – 90.8 wt% Solid – 5 wt%	
LDPE		41.5				Gas – 84.4 wt% Solid – 11.8 wt%	
HDPE		166				Gas – 87.1 wt% Solid – 11.3 wt%	
PE	20–90 µm	5	Ar – 40 slpm	RF induced – 10–20 kW 2–4 MHz	–	Gas – C_2–C_4 olefins (50 wt%)	Guddeti et al. (2000a)
PP	5–95 µm	1.5	Ar – 15 slpm	RF induced – 10–20 kW 2–4 MHz	–	Gas – C_3H_6 (78 wt%)	Guddeti et al. (2000b)
PP	20–80 µm	12–30	H_2 – 83 lpm	Rotating DC arc – 10–30 kW 80–100 A 200 V	–	Gas – C_2H_2 (77.43 wt%)	Zhang et al. (2017)

Table 2: (continued)

Feed	Particle size	Feed rate (g/min)	Forming gas	Plasma specs	Operating conditions	Output	References
PET	20–60 µm	12–20	H_2 – 62.5 – 83 lpm	Rotating DC arc – 10–30 kW 80–100 A 200 V	–	Gas – C_2H_2 (42 %), CO (53 %)	Zhang et al. (2018)
PE	200 µm	0.4	N_2 – 1 L/min	RF induced – 1.6–2 kW; 0.5–1.5 A; single set of electrodes	1.8 kW; 0.05 bar	Gas (13.67 wt%) – H_2 (10 %), CO, CH_4, C_2+ Solid	Tang and Huang (2007)
PE	<500 mm	50	N_2 – 150 L/min	DC arc – 13.5 kW	750 °C	Gas – H_2, CO Oil – C_{10}–C_{33}	Mączka et al. (2013)
MPW	30–50 mm	33.33	–	DC arc – graphite electrodes; 100–300 A	1,700–2,000 °C	Gas (75 wt%) – H_2, CO Solid (25 wt%) – slag	Mukherjee et al. (2024)
LDPE + PET						Gas (59 wt%) – H_2, CO Solid (41 wt%) – slag	

Additionally, high temperatures, along with a reducing environment, help suppress the formation and promote decomposition of hazardous compounds like dioxins and furans (Safavi et al. 2021; Tang et al. 2024). On comparison, gasification of waste produces $2 \times e^{-11}\,g/m^3$ dioxins and incineration produces $1.8 \times e^{-7}\,g/m^3$ (Yepes Maya et al. 2016). Commonly, air, pure O_2, or steam is used as the oxidizing agent, either alone or in specific ratios. In some cases, CO_2 is also employed as an oxygen source. Multiple endothermic and exothermic reactions, as shown in Equations (7)–(16), occur simultaneously within the gasifier.

$$C_nH_mO_k \rightarrow aC + bCO + cCO_2 + dCH_4 + eH_4 + fH_2O + C_xH_y + C_zH_w \ [\text{thermal cracking}] \tag{7}$$

$$C_nH_mO_k + \frac{(n-k)}{2}O_2 \rightarrow nCO + \frac{m}{2}H_2 \ [\text{partial oxidation}] \tag{8}$$

$$C_nH_mO_k + (n-k)H_2O \rightarrow nCO + \left(\frac{m}{2} + n - k\right)H_2 \ [\text{steam reforming}] \tag{9}$$

$$C_nH_mO_k + (n-k)CO_2 \rightarrow (2n-k)CO + \frac{m}{2}H_2 \ [\text{dry reforming}] \tag{10}$$

$$H_2O + CO \rightarrow CO_2 + H_2 \ [\text{water gas shift}] \tag{11}$$

$$C + H_2O \rightarrow CO + H_2 \ [\text{heterogeneous water} - \text{gas reaction}] \tag{12}$$

$$C + O_2 \rightarrow CO_2 \ [\text{combustion}] \tag{13}$$

$$CO_2 + C \rightarrow 2CO \ [\text{Boudouard reaction}] \tag{14}$$

$$C + 2H_2 \rightarrow CH_4 \ [\text{methanation}] \tag{15}$$

$$CO + 3H_2 \rightarrow CH_4 + H_2O \ [\text{methanation}] \tag{16}$$

Initiated by drying and propagated by pyrolysis, these reactions continue through gasification stages wherein pyrolysis products react with gasifying agents Equations (8)–(14). The process predominantly yields syngas, with minor amounts of tar typically present as impurities. While gasification of plastic waste shows great potential to produce H_2 and energy, the operational issues of generating up to $160\,g/m^3$ of tar as a byproduct acts as a major operational issue (Cortazar et al. 2023; Lopez et al. 2018; Mastellone et al. 2010; Wilk and Hofbauer 2013; Yousef et al. 2024). The US Department of Energy defines tar as a complex mixture of hydrocarbons having a higher molecular weight than benzene (Rabou et al. 2009). Tar formation occurs due to the random cleavage of polymeric chains, influenced by varying temperatures and residence times within the reactor. The presence of polyolefinic waste promotes the formation of light olefins, which serve as precursors for tar formation at lower temperatures. Additionally, polymers containing aromatic rings, such as PS and PET, contribute to the production of PAHs, one of the key components of tar. On an industrial scale, tar buildup poses several operational challenges, including reduced heat transfer, reactor wall corrosion, increased maintenance costs due to frequent cleaning, lower carbon conversion efficiency and energy recovery. Tar management has been practiced for decades, using both primary and secondary measures. Primary measures, such as optimized reactor design, catalytic bed materials (Han et al. 2022), and two-stage gasification (Park et al. 2016) help in tar minimization. Secondary measures, including catalytic cracking, thermal cracking, oil scrubbing, and adsorption, are then applied to achieve syngas purity suitable for downstream applications (Anis and Zainal 2011). While conventional methods remain dominant in industry, recent research explores advanced techniques such as in-line pyrolysis-steam reforming (Razak et al. 2024) to further improve efficiency. Although these methods reduce tar formation and enhance syngas quality, they often require complex setups, additional catalysts, and lower operating temperatures, which can limit the degree of plastic waste conversion. In contrast, thermal plasma gasification achieves process intensification by operating at extremely high temperatures, ensuring complete decomposition of plastic polymers, minimizing tar and toxic by-products, with greater flexibility in handling diverse waste streams. However, these outcomes are highly dependent on the reactor design, which plays an important role in determining the extent of conversion.

Throughout the reviewed literature plasma gasification has three main material inputs – the feed, oxidizing gas, and plasma-forming gas. In a few cases the plasma-forming gas acts as the oxidizing agent. However, the scenario changes with the scale, an additional input in the form coke bed is added in large scale reactors which not only acts as a mechanical support for the waste bed and a heat source or heat trap but also provides a strong reducing environment. Such conditions facilitate the reduction of refractory metal oxides (e.g., Fe_2O_3 to FeO), thereby enhancing the activity of fluxing agents and promoting slag formation (Gollapalli et al. 2024; Horton et al. 2016). The oxidizing agent can be introduced at various points along the reactor walls or via peripheral injection through the plasma torch. Injecting oxidizing gas through multiple ports or nozzles at different heights in a reactor allows for uniform gas distribution, which enhances mixing and provides control over gasification zones (pyrolysis, oxidation, reduction). Peripheral injection allows for regulated distribution around the plasma arc, leading to a higher rate of heat transfer to the oxidizing gas near the feed which can increase the rate of reaction by increasing the rate of volatilization. However, temperature distribution and electrode erosion must be carefully analyzed based on the chosen injection technique to optimize reactor performance.

Figure 3 presents a schematic of plasma gasification plant, typically the process consists of waste pre-processing units, plasma torches, gasifier, power supply, and compressors, which are then followed by the down streaming processes of char separation, gas cleaning, and purification just like other thermochemical processes. The studies on treatment of plastic waste through plasma gasification have been summarized in Table 3. The energy efficiency of the process depends on the quality of syngas produced, which is greatly affected by the oxidizing gas used. The theoretical composition of syngas produced by gasification of waste plastics using different oxidizing agents can be estimated from Equations (8)–(11) (Razak et al. 2024). Fathi et al. (2024), detailed the gasification of PP using H_2O/Ar plasma and CO_2 as the oxidizing medium; the syngas produced contained high amount of H_2 and CO, occupying 85.4 vol% of the total mixture. The authors also explored the effects of super-stoichiometric and sub-stoichiometric additions of CO_2 and reported a highest CO_2 decomposition rate of 99 % with sub-stoichiometric levels. The overall energy efficiency, considering the syngas and solid carbon, was 54 %. Hlina et al. (2014), also used CO_2 oxidizer to convert a mixture of HDPE (89 %), PP (10 %), and PET (1 %) into syngas with a LHV of 10.77 MJ/m^3 with 80 % carbon conversion to gas. This level of conversion is consistent with the use of stoichiometric amounts of CO_2, which limits complete gasification of carbon. Higher carbon conversion efficiency can be achieved under super-stoichiometric CO_2 conditions, as demonstrated by Fathi et al. (2024). Whereas Hrabovsky et al. (2010), worked with a mixture of CO_2 and O_2 as the oxidizing media, the syngas produced was reported to have an LHV of 8.5 MJ/m^3 and 100 % conversion. The difference in conversion performances in these two cases is due to the presence of O_2, and even though the amount of H_2 that can be produced theoretically is the same for both the oxidizing agents, the LHV of syngas produced through the CO_2 oxidized system is higher due to a higher occurrence of Boudouard reactions. The choice of gasifying agent – CO_2, H_2O, O_2, or air – depends on whether the goal is to maximize CO or H_2 production, optimize energy consumption, or prioritize cost-effectiveness for waste-to-energy applications. Supplementary Table S2 compares different oxidizing agents and the objectives that they serve.

3 Plasma torch

3.1 Arc plasma

Thermal plasma torches used in waste processing are classified into transferred and non-transferred types, based on the location of formation of plasma arc as shown in Figure 4. In transferred torches, the arc forms between the cathode and the conductive work piece (anode), enabling efficient heat transfer ideal for high-energy tasks like welding and metal processing. Non-transferred torches form the arc within the torch itself, projecting a high-temperature plasma jet (2000–15,000 K), making them suitable for pyrolysis and gasification of non-conductive carbon-based wastes like plastics. These torches offer greater flexibility in configuration and reactor integration. Further classification based on the power source used for plasma generation is as follows:

3.1.1 DC arc plasma

Due to their high temperature and energy density, direct current (DC) thermal plasma torches are widely used in waste-to-energy and material recovery applications. These torches utilize an electric arc formed between two high-conductivity electrodes (typically Cu, W, Hf) through which a plasma-forming gas is passed. It is important to note that the electrode material strongly influences the erosion behavior, oxygen-rich plasmas can cause rapid oxidation in Cu electrodes, whereas W or Hf provide stability and longer lifespan under such conditions (Chen et al. 2025; Ghorui et al. 2016). DC torches achieve core temperatures of 5,000–15,000 K, making them suitable for high heat flux applications. More information over the design and functioning of DC torches can be found in the works of Ghorui et al. (2010).While DC torches exhibit high efficiency and excellent durability to processing conditions, electrode erosion remains a critical limitation, requiring advanced materials and cooling systems to prolong electrode life (Szente et al. 1992). A notable advancement is the Ar–water stabilized DC plasma torch, which uses tangential water injection to stabilize the arc and generate plasma. A small flow of Ar is added to reduce cathode oxidation and enhance arc stability. This configuration achieves plasma temperatures up to 18,000 °C and specific enthalpies around 200 MJ/kg, while minimizing gas flow and syngas dilution. It incorporates a water-cooled rotating copper anode, which extends electrode life. While it requires high electrical input (80–150 kW) and robust

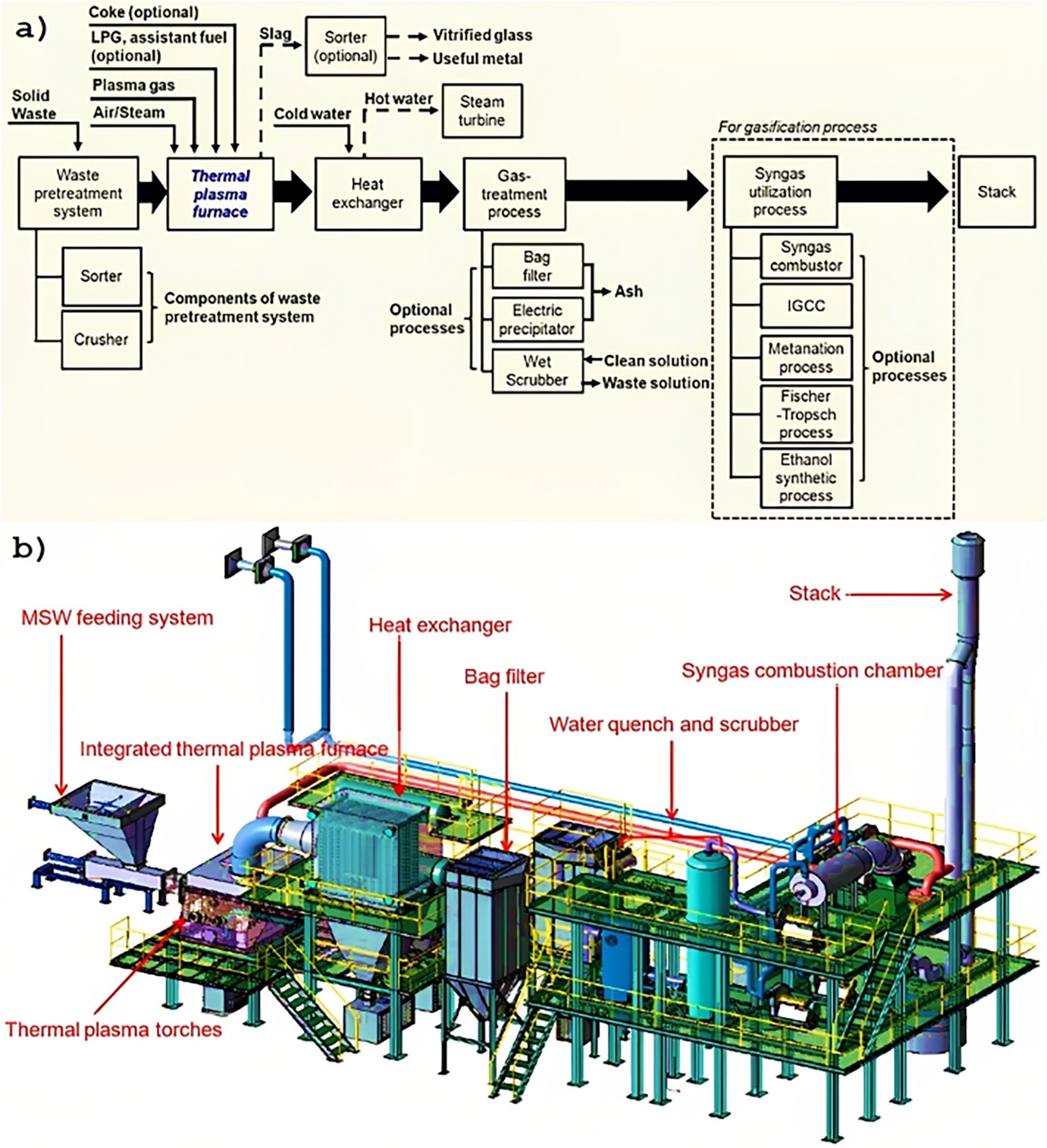

Figure 3: Plasma gasification process. (a) Block diagram representation of the plasma gasification process with upstream and downstream processes. (b) Schematic representation of 10 TPD plasma gasification plant at GS Plastech, Cheongsong, South Korea. Reproduced with kind permission from ref. (Byun et al. 2012). Copyright 2012, IntechOpen.

thermal management, it offers high heat transfer efficiency and improved operational stability. This makes it particularly suitable for plasma gasification where tar destruction and syngas quality are critical (Sikarwar et al. 2022a).

Despite this, their adaptability and ability to achieve local thermodynamic equilibrium (LTE) make them an apt option for plasma gasification systems of carbon-based waste such as plastic waste and vitrification of inorganic waste (Fathi et al. 2024; Hlina et al. 2014; Hrabovsky et al. 2010).

3.1.2 AC arc plasma

Alternating current (AC) plasma torches have emerged as an advanced technology for the thermal processing of plastic waste (Surov et al. 2017). Temperatures of 5,000–10,000 K are obtained through AC torches, facilitating the breakdown of plastic waste materials into syngas. AC plasma torches provide several advantages for waste gasification compared to DC torches, they systems have longer electrode lifetimes due to alternating polarity, reducing wear and erosion. This is

Table 3: Summary of studies on plastic waste treatment through plasma gasification.

Feed	Particle size	Feed rate (g/min)	Forming gas	Oxidizing gas	Plasma specs	Operating conditions	Output				References
							H_2 (% in gas)	CO (% in gas)	Energy efficiency (%)	Carbon conversion (%)	
PP	–	100	H_2O/Ar – 18–48 g/min	CO_2 – 76 L/min	DC arc – 95 kW	1,150–1,350 °C	40.8	44.6	54	80	Fathi et al. (2024)
PVC + biomass	0.2–2 mm	Batch – 300 g	N_2 – 36–40 L/min	H_2O	DC arc – 0 to 30 kW; 0–150 A	800 °C; S/C = 1.8; PVC – 60 wt%	47.89	25.95	–	97.57	Chu et al. (2023)
PE	–	228.3	Ar – 40 L/min	H_2O – 300 g/min	DC arc – 100 kW; 250–300 A	1st reactor – 1,400–1,500 °C; 2nd reactor – 1,200 °C; S/PE-0.9; retention time – 1.22 s	65	26	–	–	Park et al. (2006)
PE	0.2 mm	0.4	N_2 + H_2O – 0.5 L/min each	–	RF induced – 1.6–2 kW; single set electrodes	1.8 kW; 0.05 bar	6 wt%	44.6 wt%	–	25.53	Tang and Huang (2007)
Mixed plastic	Φ = 50 mm × 300 mm	16–66	–	H_2O – 50 g/min	Microwave plasma – 7.5 kW; 2.45 GHz	1,500 °C	67	7	–	97.4	Ganza and Lee (2023)
PP	–	300	Air – 1016 L/min	O_2; CO_2 – 46 L/min	Microwave plasma – 40 kW	1,400 °C	19.7	17.6	60	~52	Fathi et al. (2025)
PP + PE	Φ = 8 mm × 12 mm	173	H_2O – 246 g/min	H_2O	DC arc – 56.9 kW	2,600 °C; S/C = 1.45	49.21	~21	51.7	–	Yousef et al. (2024)
GFRP	–	0.8	N_2 – 16.5 L/min	O_2 – 1.7 L/min; H_2O – 0–0.8 ml/min	Microwave plasma – 1.8 kW; 2.45 GHz	O_2/fuel = 0.5; H_2O/fuel = 0.6; 1.4 kW	10	46	10	11	Yun et al. (2017)
PE	–	Batch – 1g	Ar + H_2O (20 mol%)	–	Microwave plasma – 0.6 kW; 2.45 GHz	Reaction time – 5 min	–	–	–	–	Sekiguchi and Orimo (2004)
PS	–	–	Air + H_2O (0–50 wt%)	–	AC arc – 500 kW; 500–1,500 A; dual torches	Plasma steam content – 51.3 wt%; 1 bar; 1,500 K	50	35	–	–	Obraztsov et al. (2019)
Plastic waste	1–6 mm	190 g/min	H_2O + Ar (18 + 12 g/min)	CO_2 – 300 L/min	Rotating DC arc – 100–110 kW	1,200–1,400 °C	41.6	49.7	–	80	Hlina et al. (2014)
PE	6 mm	95 g/min	H_2O + Ar (18 g/min + 8 L/min)	CO_2 + O_2 (210 + 80 L/min)	DC arc – 130–140 kW; 450 A;	1,560 °C	29.9	41.3	–	100	Hrabovsky et al. (2010)
PE	6 mm	176 g/min	H_2O + Ar (18 g/min + 8 L/min)	CO_2 + O_2 (210 + 80 L/min)	DC arc – 130–140 kW; 450 A	1,540 °C	35.3	41.5	–	100	Hrabovsky et al. (2010)
Plastic waste	–	–		–		1,300 °C	62.5	34.1	85	–	

Table 3: (continued)

Feed	Particle size	Feed rate (g/min)	Forming gas	Oxidizing gas	Plasma specs	Operating conditions	Output				References
							H_2 (% in gas)	CO (% in gas)	Energy efficiency (%)	Carbon conversion (%)	
			Air + H_2O (84.29 wt%)		AC arc 3 phase – 52–86 kW; 28.5 A; 1–1.8 kV						Rutberg et al. (2013)
RDF (47 % plastic)	25 mm	483 g/min	Ar – 87 L/min	H_2O – 300 ml/min	DC arc – 120 kW; 350–550 A	1,429 °C	53	30	56	~85	Agon et al. (2016)
				$CO_2 + O_2$ (177 + 93 L/min)		1,536 °C	30	46	48	~87	

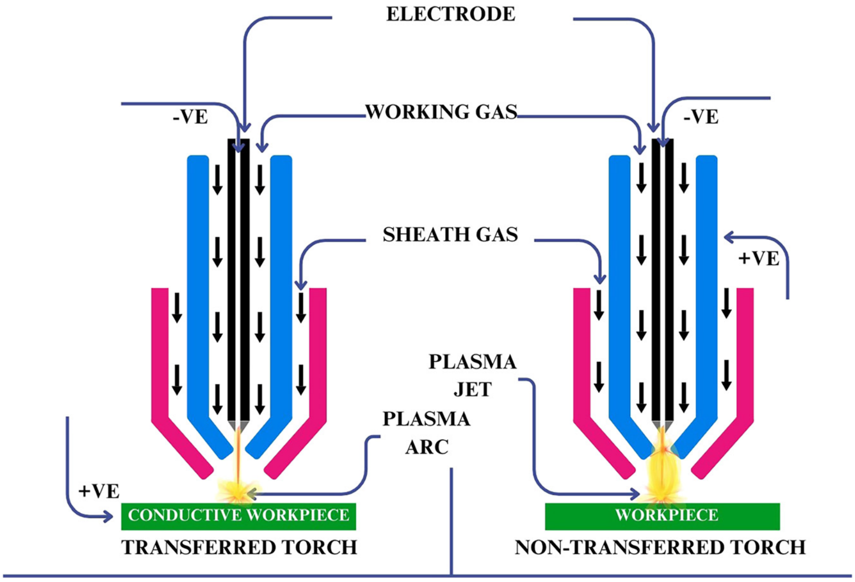

Figure 4: Schematic representation of transferred and non-transferred torches.

beneficial in reducing opex and improves operational continuity. Research highlights the efficiency of AC plasma torches, with thermal efficiencies exceeding 90 % (Obraztsov et al. 2019). Rutberg et al. (2013), demonstrated the ability novel three-phase AC plasma torch to process high-caloric waste with steam–air mixtures, and achieve syngas yields up to 3.62 m^3/kg and H_2 content exceeding 55 %. Their scalability and efficiency make them ideal for modern waste-to-energy systems but the ease of operation of DC torches make them a popular choice among industrialists.

3.2 RF induced plasma

Radio frequency (RF)-induced plasma is generated using electromagnetic induction, typically at frequencies between 13.56 MHz and 40 MHz (Gabbar et al. 2021). AC flows through an induction coil, to create oscillating magnetic fields that induces eddy currents in the forming gas. These currents ionize the gas, sustaining the plasma with electron densities of the order 10^{16}–10^{23} m^{-3} and temperatures between 6,000 and 10,000 K. Generally low enthalpy gases like Ar and N_2 are used in RF plasma torches and oxidizing gases are added in small concentrations. Their design typically features concentric quartz tubes, with the central tube supplying the plasma-forming gas and a sheath gas for cooling (Guddeti et al. 2000a,b). However, RF plasma torches are less efficient than DC systems and face challenges in gas flow rate control and power output. The complexity of ignition and maintaining stability under varying conditions necessitates precise optimization of system parameters.

3.3 MW induced plasma

Microwave-induced plasma is generated using high-frequency electromagnetic waves, typically between 300 MHz and 10 GHz, with 2.45 GHz being the most common frequency due to its availability and effectiveness in ionizing gases (Gabbar et al. 2021). These plasmas utilize electron cyclotron resonance, where electrons spiral in circular paths under a magnetic field, enabling efficient energy transfer and minimal thermal losses (Sanlisoy and Ozdinc Carpinlioglu 2019). MW plasmas are characterized by larger plasma zones and higher densities compared to RF plasmas, making them ideal for applications requiring high energy distribution over a wide area (Ho et al. 2017). However, MW plasma torches face challenges, including lower efficiency compared to DC systems and difficulties in scaling for industrial use as impedance matching and plasma stability require precise engineering (Zamri et al. 2021). Despite these limitations, MW plasma technology continues to show potential for scale-up. Supplementary Table S3 provides a comparative summary of non-transferred arc and microwave plasma torches, covering both technical and non-technical aspects in the context of waste processing.

4 Feedstock and products

4.1 Effect of feedstock on product

In thermal plasma waste processing, the relationship between the feed material and the resulting product is central to understand the efficiency and outcomes of the process.

The feed, typically consists of waste materials such as MSW or industrial residues, undergoes high-temperature transformations in the plasma reactor. This section explores various factors of feed such as composition, inorganic content, feed rate, particle size, and moisture that significantly influence the overall performance of the plasma system.

Sorting and segregation of plastic waste from other waste is difficult in countries like India (Kibria et al. 2023), leading researchers to explore plasma co-gasification of mixed waste streams as an efficient solution for managing waste while minimizing the need for complex pre-sorting steps. Park et al. (2016), studied the effect of varying blend ratios of HDPE and wood pellets on the syngas composition. The study found that increasing biomass content led to higher CO_2 concentrations, attributed to the greater oxygen content in wood. Conversely, higher HDPE content resulted in increased CH_4 production. In another plasma co-gasification study for sawdust and PVC mixtures by Chu et al. (2023), it is reported that chlorine release distribution is mainly dominated by HCl in the gas product, KCl in liquid, and $KCaCl_3$ in solid product. The proportion of total chlorine released into the gas phase increased significantly by 17 % as plasma torch power rose from 16 to 24 kW, and by approximately 6.3 % with an increase in the steam-to-carbon (S/C) ratio from 0 to 2. These findings suggest that input power (and thereby temperature) exerts a stronger influence on chlorine volatilization than the S/C ratio.

While the type of feed significantly affects the efficiency and outcomes of plasma gasification, the feed rate also directly affects residence time and thermal exposure of particles, thereby influencing gas yield and conversion efficiency. Tang et al. (2003), observed that increasing the PP feed rate from 20 g/min to 40 g/min at a fixed power input of 35.2 kW reduced the H_2 concentration in the gas from 68.8 % to 62 % and increased the yield of C_2 gases, indicating incomplete thermal cracking due to shorter residence time. Increasing the feed rate reduces the mean temperature available to heat each particle thus leading to lower conversion of solid to gas and a higher solid yield (Guddeti et al. 2000b). Zhang et al. (2017), demonstrated that while the overall carbon conversion was similar at feed rates of 12 g/min and 17.65 g/min, the higher feed rate resulted in greater acetylene yield and lower specific energy consumption, thus enhancing energy efficiency.

Volatilization of feed particles is the first stage of reaction inside the plasma processing reactor and plays an integral role in determining the overall reaction rate and efficiency of the reactor. The size of the particle controls the rate of heat transfer from plasma gas to the particle surface where the reaction initiates thus also impacting the rate of reaction. Hrabovsky et al. (2022), explains that with decreasing particle size the surface temperature of the particles increases and therefore increases the rate of gasification as illustrated in Supplementary Figures S2 and S3.

Moisture content in the feed is another critical parameter that influences plasma processing efficiency. Controlling the moisture is also important to maintain consistency in feed quality as moisture content can vary seasonally and regionally (Singhal et al. 2022). Syarif et al. (2019), modeled the temperature profile of a plasma electric furnace used for processing MSW (see Supplementary Figure S4), and reported the impact of varying feed moisture content on the temperature distribution along the reactor. As the wet feed moves through the reactor, moisture evaporates and generates steam, which acts as a sheath gas around the feed. This increases the power demand on the plasma torch to heat the feed sufficiently for gasification. Additionally, more energy is required to break down water molecules before gasification can proceed. Higher moisture content increases the steam inside the reactor which on mixing with the hot gases increases the total pressure and flowrate of gas inside the reactor that affects the residence time and overall conversion. The increase in feed moisture inversely affects the ratio output gas LHV to total reaction enthalpy, which means decreasing energy efficiency of the conversion process. In another study, it was shown that incorporating a resistively heated drying zone in the reactor reduced the specific power required for gasification by the plasma torch to 0.4 kWh/kg (Aliferov et al. 2016). Therefore, pre-drying the feed, whether through resistive heating or by recycling heat from the product gas can significantly improve process efficiency.

4.2 Effect of plasma-forming gas

The plasma-forming gas, combined with a carrier gas or oxidizing agent, creates the reactive environment necessary for plasma waste processing. Plasma can serve either as a heat source alone or as both a heat source and reactive medium, depending on the specific processing technique employed, as illustrated in Figure 5. Inert gases, such as Ar and N_2, are typically used in plasma pyrolysis to prevent oxidation of the waste material. In contrast, oxidizing gases are utilized in plasma gasification, contributing additional heat through exothermic reactions, as previously discussed. When scaling up to industrial applications, the selection criteria for plasma-forming gases become broader, with additional factors such as power consumption for plasma generation, cost of gas, heat dissipation, electro thermal efficiency, and most importantly electrode erosion rate. Electrode erosion rate is an important factor to consider in the economics and maintenance of plasma gasification systems. The choice of gas will affect the frequency of electrode replacement and associated downtime and costs. RF and MW-induced plasma torches avoid the issue of electrode erosion. However, for large-scale waste plasma processing, water-cooled DC/AC arc torches with hollow copper electrodes are commonly used. Economical gases like steam and air are commonly used as plasma-forming gases. While steam enhances syngas quality by increasing hydrogen yield, air is more economical but dilutes the syngas due to its high nitrogen content. The downside, however, is that these gases accelerate cathode erosion by forming oxides and other intermediates with the copper electrodes, in addition to the standard erosion caused by Joule heating and ion–cathode interactions (Subbotin et al. 2018). The cathode erosion rate increases proportionally with plasma torch power and plasma residence time. Szente et al. (1992), provide a comprehensive database on electrode erosion rates for commonly used plasma-forming gases and their mixtures, all measured at a fixed flow rate of 20 L/min. The high-speed projection of eroded cathode particles may also damage the inner refractory lining. Additionally, the thermodynamic properties of plasma-forming gases significantly influence process efficiency. For example, H_2 plasma, which has been studied for acetylene production via reductive pyrolysis (Zhang et al. 2017, 2018), induces severe electrode erosion due to its high enthalpy, requiring higher power input for ionization. Figure 6a presents the enthalpy of various plasma-forming gases at different temperatures.

The high thermal conductivity of H_2, even at low temperatures (see Figure 6c), leads to elevated arc voltages, amplifying cathode erosion. As a result, H_2 is typically used in mixtures with Ar to mitigate these effects (Munz and Habelrih 1992). In contrast, Ar and N_2 typically exhibit lower specific enthalpy under plasma conditions compared to gases like steam and air. As a result, higher flow rates of Ar and N_2 are required to deliver equivalent energy for effective waste conversion, increasing gas volume and diluting the product syngas, raising downstream purification demands and raw material costs. Steam plasma, by comparison, can transfer the same energy with a lower mass flowrate and offers high thermal conductivity even at lower temperatures, promoting efficient heat transfer to the waste. However, steam's high heat capacity requires greater electrical energy input to reach plasma temperatures. Thus, another criterion, the cost of the plasma-forming gas, becomes especially critical at pilot and industrial scales, where large volumes are used continuously. Inert gases like Ar and He, though chemically stable and less erosive, are significantly more expensive than air or steam, impacting long-term operational expenses. Even steam, despite being derived from water, involves costs related to generation and system integration. Therefore, cost-effectiveness, alongside thermophysical properties, often dictates the final choice of plasma gas in scaled-up systems (Hrabovsky et al. 2022). Table 4 compares various plasma-forming gases in terms of their performance and effectiveness in waste plasma processing.

4.3 Solid product and its characterization

Thermal plasma processing of carbonaceous waste yields two categories of solid products: vitrified slag and carbonaceous residues. These products differ significantly in their origin, composition, behaviour in the reactor, and post-treatment applications. Independent discussion on these outputs is covered in this section.

Vitrified slag, often referred to as plasma rock, is a dense, glassy solid formed during plasma treatment of inorganic-rich waste streams. In plasma reactors, especially fixed-bed configurations, the inorganic components in the feed – such as metals, ash, minerals, and glass – melt under extreme temperatures and exit the reactor as a molten flow. Upon rapid cooling or quenching, this flow solidifies into a vitrified structure that encapsulates hazardous elements. The stability, structure, and leaching behavior of this slag are central to its environmental safety and potential for reuse. With waste sorting and segregation being one of the toughest issues at hand in managing solid waste, it is clear that the plastic waste would be sourced from municipal and medical solid waste both of which often contain significant amounts of inorganic substances in the form of glass, metallic entities, and mineral waste (Sniadecka et al. 2016). Chu et al. (1998), conducted thermal plasma processing experiments using synthetic medical waste surrogates consisting of both combustible (e.g., pork ribs, gauzes, swabs) and non-combustible (e.g., stainless steel, glass, syringes) fractions. The study highlights that when metallic components exceed the 40 wt% limit in feed, the resulting slag could surpass regulatory leaching thresholds for heavy metals. Therefore, a careful balance in the inorganic fraction is essential. To promote proper melting and glass formation, fluxing agents – primarily CaO, SiO_2, and Al_2O_3 – are typically added to the feed. These oxides reduce the viscosity and melting point of the slag, supporting the formation of a homogenous, amorphous matrix. The recommended ranges for CaO (20–35 wt%) and SiO_2 (30–60 wt%) in the solid slag were given by Ma et al. (2021). Coke is also often included to create a reducing environment that enhances the behavior of fluxing agents and facilitates melting. Another significant factor is the cooling rate of the molten slag. Rapid quenching rates, typically above 700 °C/s, inhibit crystallization and yield a

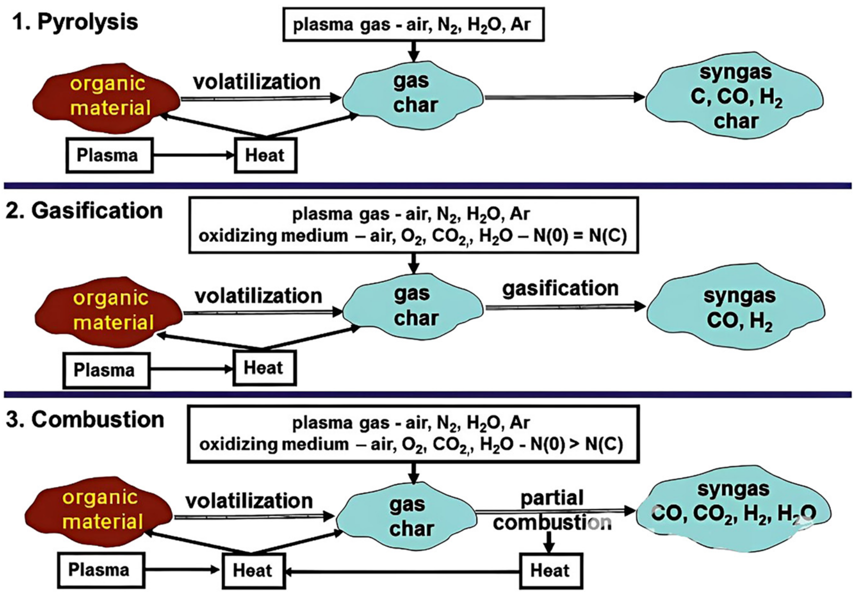

Figure 5: Selection of plasma-forming gas and carrier gas. Reproduced with permissions from ref. (Hrabovsky and van der Walt 2018). Copyright 2018, Springer.

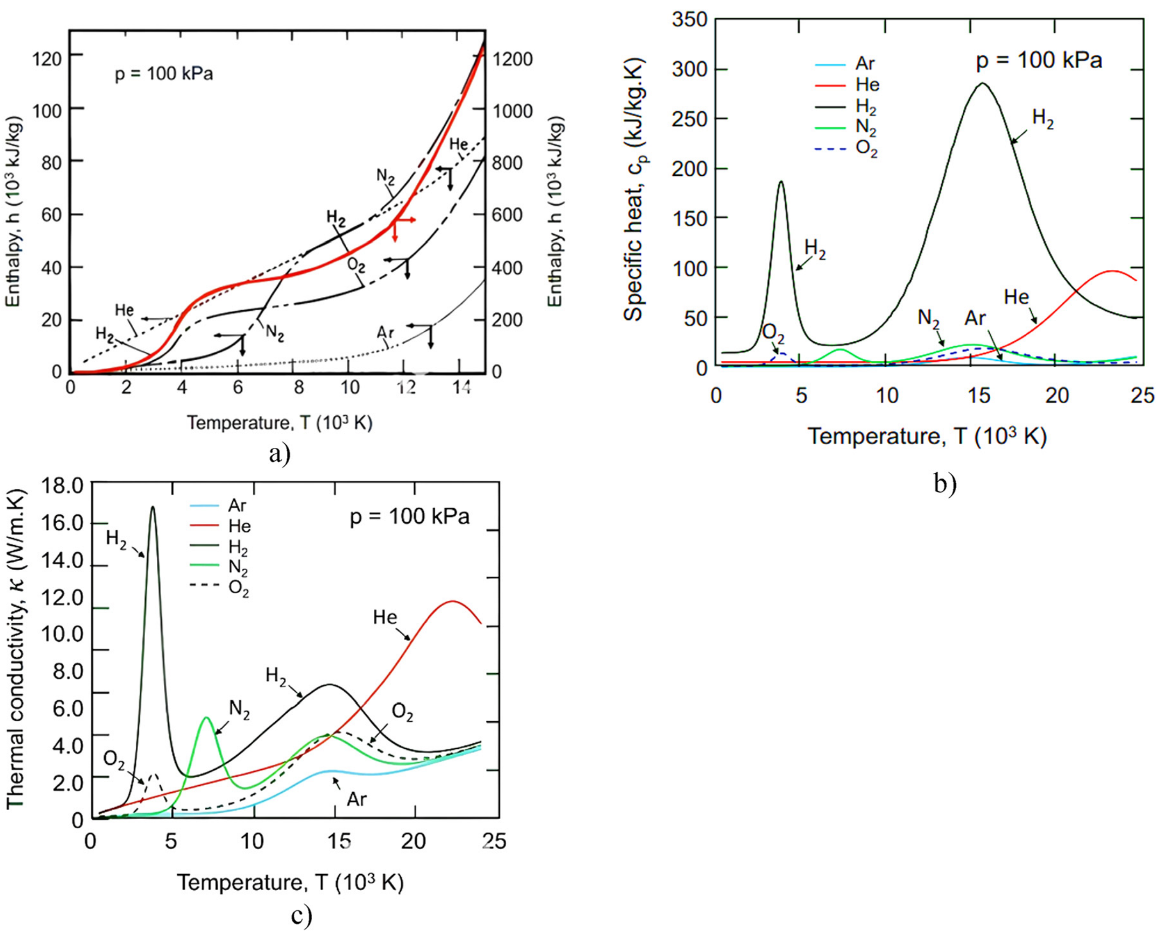

Figure 6: Thermodynamic properties of various individual gases under plasma conditions: (a) Enthalpy, (b) specific heat capacity, (c) thermal conductivity. Reproduced with kind permission from ref. (Boulos et al. 2016a).

Table 4: Comparison of plasma-forming gases for their suitability in waste plasma processing.

Forming gas	Enthalpy (specific energy content)	Specific heat (energy storage)	Thermal conductivity (heat transfer)	Electrode erosion rate	Suitability for plasma processing
Ar	Low (lack of dissociation energy and low ionization energy)	Low (does not store much energy)	Very low (poor heat transfer)	Low: argon provides a stable arc with minimal electrode wear, contributing to longer electrode life	Good for localized, stable plasma with minimal heat loss. Ideal for maintaining high temperatures without dissipating heat
O_2	Moderate	Moderate	Moderate	Moderate: oxygen can increase erosion due to reactivity, leading to oxidation of electrode materials	Widely used for oxidation reactions to boost gasification efficiency and add energy through exothermic reactions
N_2	Moderate	Moderate	Moderate	Moderate: nitrogen plasmas generally cause low to moderate electrode wear, less reactive than oxygen	Useful for controlling and balancing plasma reactions; provides thermal stability, often in combination with other gases
He	High (high energy required to ionize)	Low	High (very efficient heat transfer)	Low: helium's inert nature results in very low electrode erosion, making it ideal for long-lasting plasma operations	Excellent for high-temperature processes but not cost-effective for gasification; suitable for specialized, high-energy uses like feed with high metallic content
H_2	Very high	High (can store a lot of energy)	High	High: hydrogen causes significant electrode erosion, particularly in metals like tungsten, due to high reactivity and tendency to cause sputtering and ablation	Highly reactive; promotes efficient gasification and high syngas yields (H_2 + CO); suitable for advanced plasma systems
Air	Moderate	Moderate	Moderate	Moderate: similar to nitrogen, air plasma causes moderate electrode erosion, but the oxygen content in air can increase wear.	Most economical gas option for plasma gasification; used widely in large-scale setups
Steam	High	High	Moderate	High: steam plasma leads to significant electrode erosion, as high temperature and reactivity of water vapor cause material loss	Highly effective for enhancing gasification and increasing hydrogen output in syngas production; often used with other gases

While Ar, N_2, and air are common plasma-forming gases, they can dilute the syngas, which affects its composition for downstream synthesis processes. Additionally, inert gases like Ar and He add considerable operational cost. These factors make it crucial to carefully select both the type and amount of plasma gas in waste-to-energy applications.

dense amorphous glass, as shown by Hu et al. (2023). This rapid solidification minimizes porosity and stabilizes toxic metals, such as Cr, reducing their leached concentrations to as low as 0.002 mg/L, well below regulatory limits.

The physical properties of the resulting slag directly influence its suitability for reuse. High concentrations of amorphous oxides contribute to low porosity and high density, making the material appropriate for construction bricks, asphalt filler, or concrete aggregates (Zhao et al. 2024). Conversely, the inclusion of carbonates or sulfates – such as $CaSO_4$ – can introduce foaming effects during vitrification, producing porous slag with thermal conductivity as low as 0.22 W/m K, suitable for insulation materials (Lázár et al. 2018). Additionally, the formation of metallic inclusions (e.g., spheroidal or needle-like structures) can increase slag density and impact mechanical performance (Chu et al. 1998).

Environmental compliance is gauged through leachability testing, which assesses the long-term stability of heavy metals within the slag. The leachability of slag can be tested by a three-step sequential extraction procedure developed by the Commission of the European Communities Bureau (BCR) (Tessier et al. 1979). After the extraction, the concentration of heavy metals in each fraction of the slag is determined using an inductively coupled plasma optical emission spectrometer (ICP-OES).

The properties and type of solid product formed depend on the plasma processing technique used due to the operating conditions. In plasma gasification the amount of char and volatiles found in the solid residue is less compared to plasma pyrolysis primarily due to the oxidizing environment and higher temperatures. Bhatt et al. (2024), reported that during plasma pyrolysis of plastic waste the solid residue decreases with increase in temperature. On comparison of different polymers, PET produces the highest amount of solid residue due to formation of oxygenated compounds as previously discussed. Fazekas et al. (2016), observed that the high velocity of the plasma jet can cause solids to become entrained as soot in the off-gas and to adhere to reactor walls. This phenomenon occurs when particles spend insufficient time in the plasma zone, leading to incomplete conversion. Gas chromatography-mass spectrometry (GC-MS) analysis of compounds extracted from soot using toluene revealed that aromatic and polyaromatic compounds formed during breakdown adsorb onto the soot. Thus, optimizing residence time and maintaining temperature uniformity in the reactor are essential. Plasma pyrolysis of plastics has been explored for producing high-value carbon nanostructures as solid products. Polypropylene (PP), for example, has been studied as a feedstock for synthesizing carbon nanotubes (CNTs) through plasma pyrolysis. Transmission electron microscopy (TEM) analysis confirmed that increasing arc current decreases the diameter of the resulting CNTs (Mohsenian et al. 2018). However, despite the successful formation of carbon nanostructures observed through various microscopic techniques, the yield remains limited (up to 20 wt%), and the selectivity is insufficient for scalable CNT production via plastic plasma pyrolysis (Fathi et al. 2024).

Raman spectroscopy of the solid residue provides insight into the purity of the carbon nanostructures produced. For carbon black samples from PP plasma pyrolysis, an I_D/I_G ratio of 0.96 indicates a high degree of structural defects, such as vacancies, edge irregularities, and lattice distortions. This level of disorder could be advantageous in applications needing defect-rich surfaces, like battery electrodes, but is less ideal for applications requiring structural integrity. The CNTs synthesized through this method show limited selectivity and contain various impurities. High-resolution transmission electron microscopy (HRTEM) reveals additional carbon forms, including onion-like, spherical, and non-spherical nanostructures, which act as impurities. Furthermore, energy dispersive X-ray (EDX) analysis highlights the presence of inorganic elemental species within the solid residue, further impacting the purity of the final product. Mohsenian et al. (2016), found that increasing arc current during ABS pyrolysis reduces SiO_2 and $CaCO_3$ intensities in XRD spectra, indicating higher-purity carbon black at elevated power levels.

5 Engineering aspects of plasma reactor for plastic waste treatment

Understanding chemical engineering aspects like heat and mass transfer mechanisms, reaction kinetics, and hydrodynamics is essential for designing efficient plasma reactors for plastic waste treatment. Heat transfer ensures uniform high temperatures necessary for complete plastic decomposition, while mass transfer optimizes the interaction of reactants, aiding syngas production. Reaction kinetics provide insights into the rates of decomposition and gasification, guiding the selection of operating conditions for maximum efficiency. Hydrodynamics governs the flow of gases and molten slag, minimizing dead zones and ensuring proper mixing. Mastering these aspects is crucial for maximizing energy utilization, reducing emissions, and producing high-quality syngas and stable slag.

5.1 Heat transfer

Heat transfer in plasma processing of waste differs significantly from conventional processes due to the extreme temperatures, high energy densities, and unique interactions between plasma gases and waste particles, plasma systems involve complex interactions like rapid convection and potential radiative effects, requiring tailored study for accurate and efficient processing (Demchenko et al. 2019; Elaissi and Alsaif 2023; Pancholi et al. 2022).

In a plasma processing reactor, the heat required to carry out the waste conversion is provided by the plasma torch. However, the total power exerted by the torch ($P_{\mathrm{net}}^{\mathrm{plasma}}$) is the remainder value from the difference between the actual power supplied to the torch (W) and the power lost due to the heating of the torch ($P_{\mathrm{loss}}^{\mathrm{torch}}$). The power required to form the plasma is proportional to the enthalpy of the forming gas used and the capacity of the system, as represented in Equation (18) where H_{AV} is the mass-averaged enthalpy of forming gas and M is the mass flowrate (Hrabovsky et al. 2022). Looking at Equation (19) the heat delivered by the torch gets utilized for heating and volatilizing the plastic waste ($P_{\mathrm{volat}}^{\mathrm{org}}$) in the feed and melting the inorganics ($P_{\mathrm{melt}}^{\mathrm{inorg}}$). Post conversion to gas, the term $P_{\mathrm{react}}^{\mathrm{gas}}$ represents power of chemical reactions which can either be positive or negative owing to extent of endothermic or exothermic reactions. Furthermore, the power is also dissipated through the reactor walls ($P_{\mathrm{heat}}^{\mathrm{wall}}$), for reduction of which thick refractory lining is necessary. The heat is also consumed in heating the carrier gas or oxidizing gas $P_{\mathrm{heat}}^{\mathrm{oxi/carr}}$ that enter the reactor through reactor walls. Products of the conversion along with unreacted plasma leaving the reactor also dissipates heat from the system. Hence, although the heat is provided by the torch, there are several factors such as reactant flow rates, thermal conductivity of refractory lining, residence time of gases, and thermodynamic properties of plasma that control the temperature inside the reactor.

$$W = P_{\mathrm{net}}^{\mathrm{plasma}} + P_{\mathrm{loss}}^{\mathrm{torch}} \tag{17}$$

$$P_{\mathrm{net}}^{\mathrm{plasma}} = M \cdot H_{\mathrm{AV}} \tag{18}$$

$$\begin{aligned} P_{\mathrm{net}}^{\mathrm{plasma}} &= P_{\mathrm{melt}}^{\mathrm{inorg}} + P_{\mathrm{out}}^{\mathrm{slag}} + P_{\mathrm{volat}}^{\mathrm{org}} + P_{\mathrm{out}}^{\mathrm{gas}} + P_{\mathrm{react}}^{\mathrm{gas}} + P_{\mathrm{heat}}^{\mathrm{wall}} \\ &\quad + P_{\mathrm{heat}}^{\mathrm{oxi/carr}} + P_{\mathrm{out}}^{\mathrm{plasma}} \end{aligned} \tag{19}$$

In waste thermochemical conversion systems, the time constants for gas phase reactions are contrastingly shorter when compared to the volatilization of feed material which makes it significant for determining the rate of conversion. Therefore, it is important to understand the heat transfer routes and the factors affecting the rate of heat transfer to the feed.

Convection is the dominant mode of heat transfer to feed in waste plasma processing as the hot plasma comes into direct contact with waste particles transferring heat through forced convection due to high-velocity plasma flow. Radiation plays a role in both heating the waste particle and dissipating heat from the system. However, radiative heating of particle is considered negligible with the consideration that the plasma is optically thin, and angle of incidence is low, meaning that radiation can escape without significant reabsorption (Boulos et al. 2016a). That said, there are certain cases where plasma radiation does become significant which will be discussed in detail in the sub-Section 5.1.2. The loss of heat from particle surface through radiation is particularly notable for particles with high melting point such as metals and inorganics. In contrast materials with a prevailing organic structure tend to volatilize quickly and hence follow a different route. As a result, any heat distribution model must account for the concentration of organic and inorganic species in the mixed feed to accurately predict heat transfer behavior within the plasma reactor. Regarding conduction, this mode of heat transfer is mainly relevant for inorganic materials. It occurs as internal conduction, transferring heat from the particle surface to its center and is highly dependent on the thermal conductivity of the material. The modes of heat transfer between plasma, waste particle, and the reaction environment are schematically represented in Figure 7. The net heat received by a particle, Q_{net} is given by Equation (20) which is a sum of the heat received through convection, Q_{convec} , heat received through radiation from plasma, $Q_{\mathrm{rad}}^{\mathrm{plasma}}$, and heat dissipating through radiation from particle surface, $Q_{\mathrm{rad}}^{\mathrm{particle}}$, which are given by Equations (21)–(23), respectively.

$$Q_{\mathrm{net}} = Q_{\mathrm{convec}} + Q_{\mathrm{rad}}^{\mathrm{plasma}} - Q_{\mathrm{rad}}^{\mathrm{particle}} \tag{20}$$

$$Q_{\mathrm{convec}} = h \cdot A_{\mathrm{p}} \cdot (T_{\infty} - T_{\mathrm{p}}) \tag{21}$$

$$Q_{\mathrm{rad}}^{\mathrm{plasma}} = \epsilon \cdot \sigma \cdot A_{\mathrm{p}} \cdot \left(T_{\infty}^{4} - T_{\mathrm{p}}^{4}\right) \tag{22}$$

$$Q_{\mathrm{rad}}^{\mathrm{particle}} = \epsilon \cdot \sigma \cdot A_{\mathrm{p}} \cdot \left(T_{\mathrm{p}}^{4} - T_{\mathrm{w}}^{4}\right) \tag{23}$$

Here, A_{p}, ϵ, σ, represent the surface area of the particle, emissivity and Stefan-Boltzman constant, respectively. T_{∞} is the temperature of the bulk plasma phase, T_{p} is the surface temperature of the particle, T_{w} is the ambient wall temperature, and h is the heat transfer coefficient which can be calculated as shown in Equation (24) by using Nusselt number (Nu) which is most commonly a function of Reynolds (Re) and Prandtl (Pr) number, but corrections to the equation exist when the composition along with thermodynamic and transport properties of plasma are accounted for (Boulos et al. 2016a).

$$h = \frac{k \cdot \mathrm{Nu}}{D_{\mathrm{p}}} \tag{24}$$

$$\mathrm{Nu} = 2 + 0.6 \cdot \mathrm{Re}^{\frac{1}{2}} \cdot \mathrm{Pr}^{\frac{1}{3}} \tag{25}$$

Here, k and D_{p} are the thermal conductivity of plasma-forming gas and the particle diameter respectively.

Demchenko et al. (2019), studied steam plasma gasification of carbonaceous feed (coal particles in particular) by using a modified version of Equation (20) and calculated the time required for heating the particle up to the reaction temperature. Their calculation was based on common assumptions typically applied to entrained flow gasifiers – such as uniform spherical particle shape, negligible internal temperature gradients, and dominant convective heat transfer from the gas to the particle surface. However, they also noted that in the plasma gasification environment, where gas temperatures exceed 2,000 K, radiative heat transfer becomes the dominant mechanism. This suggests that such assumptions may not hold under plasma conditions, and heat transfer dynamics in plasma reactors may differ significantly from conventional entrained flow systems. The equation is given as follows:

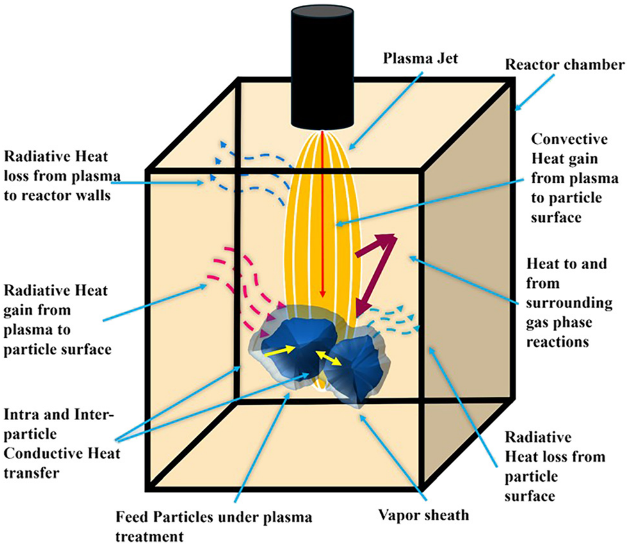

Figure 7: Heat transfer routes inside a waste plasma processing reactor.

$$\frac{\mathrm{d}T_\mathrm{p}}{\mathrm{d}t} = \frac{6\mathrm{Nuk}}{c_\mathrm{P}\rho_\mathrm{p}D_\mathrm{p}^2}(T_\infty - T_\mathrm{p}) + \frac{6\sigma\epsilon_\mathrm{P}}{c_\mathrm{P}\rho_\mathrm{p}D_\mathrm{p}}\left[\left(\frac{T_\infty}{100}\right)^4 - \left(\frac{T_\mathrm{p}}{100}\right)^4\right] \tag{26}$$

where ρ_p, and c_P represent the density and specific heat capacity of the particle respectively.

The heat transfer to carbon feed is divided into three stages, (i) heating of the particle, (ii) volatilization of particle surface and sheath gas formation, (iii) conversion to coke. Upon integrating the convection and radiation terms in Equation (26) individually we get the time required for heating the particle (t_h)

$$t_\mathrm{h} = \frac{c_\mathrm{P}\rho_\mathrm{p}D_\mathrm{p}^2}{6\mathrm{Nuk}} \cdot \ln\left(\frac{T_\infty - T_{\mathrm{p}_0}}{T_\infty - T_\mathrm{p}}\right) \tag{27}$$

$$t_\mathrm{h} = \frac{c_\mathrm{P}\rho_\mathrm{p}D_\mathrm{p}}{6\sigma\epsilon_\mathrm{P}\varphi} \cdot \frac{1}{4T_\mathrm{r}^3} \cdot \left\{\ln\left(\frac{(T_1 + T_\mathrm{r})(T_\mathrm{r} - T_0)}{(T_\mathrm{p} - T_1)(T_\mathrm{r} + T_0)}\right) + 2\tan^{-1}\frac{T_1}{T_\mathrm{r}} - 2\tan^{-1}\frac{T_0}{T_\mathrm{r}}\right\} \tag{28}$$

The heating time of coal particles, t_h is calculated using a consecutive approximation method. The convective heating temperature, T_pc, is first determined from Equation (27). Through this the radiative heating component is estimated as $T_1 = 1800 - T_\mathrm{pc}$. The t_h, value is then refined by solving Equation (28). The process iterates until convergence, effectively modeling combined convective and radiative heat transfer during gasification. As previously discussed, the time required for conversion is directly proportional to the particle size and inversely proportional to temperature of the particle. The same pattern is observed from the modelled calculations depicted in Figure 8a. Smaller particles heat faster due to their higher surface area-to-volume ratio, which accelerates both convective and radiative heat exchanges. Notably, as $T_\mathrm{g} > 3{,}000$ K, the rate of heating time reduction slows due to reduced thermal conductivity, attributed to the disassociation of water molecules. Figure 8b depicts the relationship between reactor chamber volume, V (L) and T_g for various particle sizes given by Equation (29). The graph indicates that for particles up to 50 µm, the required chamber volume does not change significantly beyond $T_\mathrm{g} = 2{,}000$ K. Larger particles ($D_\mathrm{p} \geq 150$ µm) demand significantly higher chamber volumes at all temperatures, reflecting their longer heating and conversion times. The chamber volume decreases as T_g increases up to 3,000 K, due to elevated thermal conductivity, accelerated reaction rates and faster particle conversion. These insights are crucial for optimizing reactor design, balancing temperature, particle size, and reactor capacity.

$$V = \frac{t_\mathrm{h} m_\mathrm{g} \mathrm{R} \mathrm{T}_\mathrm{g}}{P_\mathrm{g}} \tag{29}$$

where, m_g, R, and P_g are mass of gas, gas constant, and pressure inside the reactor.

The model incorporated temperature-dependent thermal conductivity of plasma-forming gas enabling detailed analysis of the prevalent mode of heat transfer in different regions of the reactor and the required time to heat the waste particle. This information is valuable in deciding the dimensions of plasma and freeboard regions of the reactor. Moreover, the reactor dimensions will vary based on the type of plasma-forming gas used, owing to the differences in their physical and thermal properties. However, the model has certain limitations, including the assumption of 1,800 K as the CBP (carbon boundary point – a temperature value beyond which carbon will not exist in solid form), the exclusion of energy exchange from gas-phase reactions which will also influence the particle heating time. Additionally, a higher valued range of particle sizes (2–50 mm) can be explored to imitate real world conditions.

5.1.1 Role of mass transfer

As the plastic waste particle heats up volatilization begins at the surface of the particle, the vapors from the moisture and more importantly the breakdown of the material form a sheath or boundary layer around the particle where the vapor concentration is higher than the surrounding bulk gas, this layer hinders with the convective heat transfer, but hardly affects the radiative heat transfer. As the reaction progresses the boundary layer thickens with continued degradation of material. Consequently, the vapors must

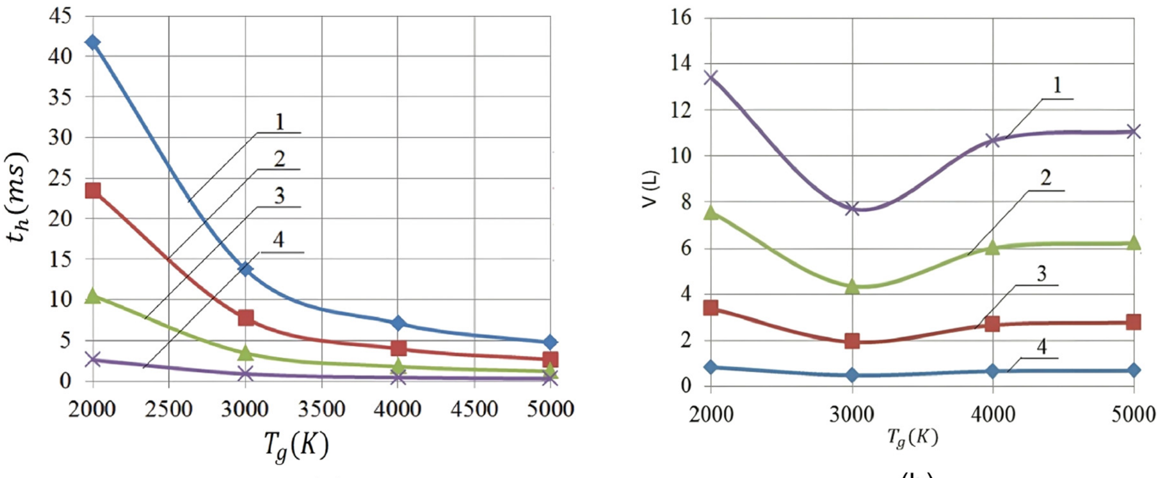

(a) (b)

Figure 8: Effect of particle size and reactor gas temperature on (a) heating time, (b) required reaction volume at constant pressure. 1 – D_p = 200 μm; 2 – D_p = 150 μm; 3 – D_p = 100 μm; 4 – D_p = 50 μm. Reproduced with kind permission from ref (Demchenko et al. 2019). Licensed under CC BY 4.0.

diffuse through the thickening boundary to reach the bulk gas phase. At this stage, heat transfer becomes mass transfer-controlled, as the rate of heat delivery to the particle surface is limited by the diffusion of degradation products through the boundary layer. This resistance due to mass transfer increases with the size of particles as the heat flux through the sheath decreases (Zairin et al. 2024; Zhang et al. 2024).

Syarif et al. (2019), demonstrated the significant impact of chemical reactions on heat transfer in plasma furnace gasification of MSW. Their model, accounts for exothermic reaction energy which results in a notable temperature increase in the gasification zone of the plasma shaft furnace, where reactions release the most heat. This leads to a spike in waste particle temperature, while the gas phase temperature remains largely unaffected, indicating that the reactions heat the waste particles. Without considering reaction energy, the waste particles' temperature profile is lower and more uniform, lacking the dynamic heating essential for efficient gasification. Domarov (2020), provides a more elaborate explanation of the model. This comparison underlines the critical role of reaction-induced energy in accurately calculating the thermal energy requirement and optimizing furnace performance. Shevchenko et al. (2024), considered the energy exchange from gas-phase reactions to estimate the residence time of particles within a steam plasma gasification reactor, subsequently using this data to determine the reactor's volume and dimensions. However, the model does not compute the mass transfer resistance offered due to the sheath layer by excluding the mutual diffusivity coefficient of gases and the volatiles from particle surfaces, by assuming the gasification process to be instantaneous within the plasma region. They further presumed the particle mass remains constant until reaching plasma temperature. This assumption, while simplifying calculations, may lead to inaccuracies in measuring the gasification rate due to the shrinking size of the particle and the temperature gradient present along the reactor length. However, these inaccuracies can be mitigated by ensuring adequate mixing of plasma with other components inside the reactor, which promotes isothermal conditions and enhances reaction consistency.

Uniform distribution of plasma in a plasma gasifier ensures consistent heat transfer, leading to efficient and complete breakdown of waste materials. This uniformity minimizes hotspots and cold zones, enhancing reaction control and reducing the risk of incomplete gasification or reactor damage. Astashov et al. (2018), proposed a novel solution using a rotation rotor to create peripheral plasma vortex flow to distribute the plasma radially. Their study showed that with the installation of a rotor the mass flux of particles was stabilized within the range of 3–4 g/m^2 min at 2,000 rpm along the reactor length. The radial distribution of isotherms also changed with the rotor speed, the length of high temperature zones covered the complete length of the reactor at 3,000 rpm compared to only 35 % length without the rotor. Therefore, inducing a peripheral plasma vortex reduces the cold zones inside the reactor.

5.1.2 Radiation

Radiative heat transfer is generally neglected in waste plasma processing systems due to the complexity of the calculations involved. However, radiation occurs through the plasma, the solid particles within the system, and the refractory lining which absorbs and re-radiates heat depending on its emissivity and temperature. Waste plasma processing reactions are mostly performed at atmospheric pressure and with an arc temperature range of 5,000–15000 K where the effects of radiation are subdued. Nevertheless, the thermodynamic properties of plasma change at high pressures, currents and temperatures. Diab et al. (2024), in their work explain that plasma at 1 bar can dissipate significant amounts heat at currents higher than 100 A and at higher pressures such as 20 bar it becomes optically thick as the plasma density increases and even emit and absorb radiation at lower current values. Figure 9 shows how the increasing trend of axial temperature varies with and without accounting for radiation in the model as pressure and current values are increased for a hydrogen arc plasma. Plasma arc torches generally operate in the range of 100–1,500 A as seen in the studies listed previously in Tables 2 and 3 indicating at the possibility of heat dissipation through radiation inside the arc chamber and loss of power to torch that can reduce the electro thermal efficiency. The practical ranges for significance of radiative plasma are as follows:

- Insignificant radiation: current < 100 A, pressure < 1 bar, temperature < 10,000 K.
- Significant radiation: current > 100 A, pressure > 10 bar, temperature > 15,000 K.
- Dominant radiation: current > 200 A, pressure > 50 bar, temperature > 20,000 K.

Upon plasma – solid interaction inside the reactor the heat loss due to radiation becomes more prominent with increasing surface temperature, surface area, and the melting point of the solid. When then particle size of materials such as metals increases the temperature of plasma required to melt the particle also increases as it continues to lose heat through radiation (Boulos et al. (2016a). The temperature increase is however subjective to the thermal conductivity of the forming gas. The inclusion of radiation heat transfer in numerical models of plasma reactors significantly influences the accuracy of predicted outcomes, such as temperature distribution, soot formation, and gas concentrations. Liavonchyk et al. (2021), using an entrained-flow plasma gasifier, compared the simulated and experimental results for plasma gasification of rubber pyrolysis vapors and demonstrated that accounting for radiation improved temperature predictions, reducing discrepancies between modeled and experimental values. Without radiation, temperatures at various points in the reactor were substantially overestimated, with deviations of up to 470 K. Incorporating radiation reduced these errors to a range of 100–180 K. The errors arose due to the inaccuracy in assigning the radiation model to the fibrous insulation refractory material in the reactor. In a similar previous study, Liavonchyk et al. (2017) stated that the inaccuracies were a result of defining the properties of refractory material as independent of temperature and also due re-radiation from walls.

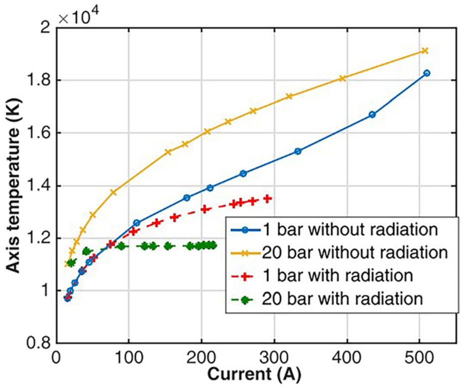

Figure 9: Axis temperature of wall stabilized hydrogen arc column with and without radiation at 1 bar and 20 bar. Reproduced with kind permission from ref. (Gueye et al. 2017). Copyright 2017, AIP Publishing.

Soot formation also varied significantly with the inclusion of radiation effects. In Liavonchyk et al. (2021), models without radiation over-predicted soot content at 6.7 wt%, whereas models with radiation reduced this to 2.9 wt%, aligning better with experimental trends. This reduction is attributed to improved heat distribution, which enhances soot oxidation into syngas. It is further emphasized that accurate modeling of soot kinetics remains challenging due to thermodynamic equilibrium simply not allowing the formation of soot at high temperatures and the employed models being more accurate for complete combustion reaction mechanisms while only being nearly approximate for partial oxidation reactions (Liavonchyk et al. 2017). These findings underscore the critical role of radiation in enhancing model reliability but also point to areas needing further refinement.

5.2 Theoretical studies

Thermal plasma processing of waste demands extremely high temperatures, resulting in significant electricity consumption and a large supply of plasma-forming gas at elevated pressures. Additionally, frequent maintenance of plasma torches further increases the cost of collecting data through experiments. The process is also highly time-consuming due to the need for optimizing multiple variables, such as feed flow rate, gas flow rate, temperature, pressure, plasma torch configuration, and the type of forming gas used. Therefore, to increase the pace of attaining technological maturity mathematical models are developed (Munir et al. 2019). Mathematical models can be of three types namely – equilibrium, numerical, and kinetic. Equilibrium models also known as systematic models are a simpler approach to predict the outcomes of a process based on minimization of Gibb's free energy and by assuming a thermodynamic equilibrium (Janajreh et al. 2013; Montiel-Bohórquez et al. 2022; Pitrez et al. 2023; Sharma 2008). Accurate prediction of output is necessary to design the down streaming processes. Equilibrium models do not take into account the effects of reactor geometry, heat and mass transfer patterns, reaction kinetics, and assume infinite residence time which results in lack of validation from experimental results. Most studies published on non-stoichiometric Gibb's free energy minimization approach provide data with the assumption of an idealized behavior, which is impractical and insufficient in reactor designing. On the other hand, Numerical models consider flow equations, reactive species, and reactor geometry to solve complex equations of heat, mass, and momentum transfer by using computational techniques. Finite element analysis (Sedej and Mbonimpa 2021), finite volume analysis (Qing et al. 2022), Monte carlo simulations, and density function theory (Huang et al. 2013) are some of the commonly reported computational techniques. Kinetic models observe the chemical reactions in a system and determine their kinetic rates. These high-fidelity models prove to be very useful in estimating the harmful pollutants such acid gases, and dioxins and furans produced during the thermal treatment of waste as they follow slow kinetics (Grandesso et al. 2008; Bei et al. 2022). These different models are discussed in depth in the sub-sections ahead.

5.2.1 Numerical models (CFD)

Computational fluid dynamics studies group together conservation of mass, energy, and momentum in a defined volume to provide a theoretical description of the process. For multiphase reactions such as plasma pyrolysis and plasma gasification, CFD is important to visualize the plasma – material interaction, heat distribution, flow and concentration of gases inside the reactor, heat transfer to the material, progression of the reaction through volatilization and describe the kinetics of homogeneous chemical reactions. Two general modelling approaches, Euler–Euler and Euler–Lagrangian have been followed by researchers to simulate multiphase plasma reactors. The Euler–Euler method uses volumetric representation to show the presence of both continuous and discrete phases in definite volumes, here both phases are treated as interpenetrating continuous phases. On the other hand, Euler–Lagrangian method analyses continuous and discrete phases separately. This approach is widely used even in conventional fluidized bed gasification to track the trajectory and interaction of individual particles. However, the high conversion rates of waste particles such as plastic in a plasma reactor raise the question as to which method will be more efficient. Popularly Euler–Euler approach has been followed mainly due to the quick conversion of solids into gas and also because fewer boundary conditions (particle size boundaries eliminated) and lesser computational power is required compared to Euler–Lagrangian. A more detailed explanation on the application of these CFD modelling approaches for thermochemical waste processing technologies in the turbulent regime is given by (Ramos et al. 2019a,b). CFD models are an economical and time efficient option for optimization of operating conditions and structure of the plasma reactor, Table 5 features CFD simulation studies carried out for waste plasma processing. Ismail et al. (2019), simulated a plasma fixed bed gasifier for processing MSW by describing kinetic reactions using Arrhenius correlation in a two-step model of primary pyrolysis to produce gases followed by tar cracking. Homogeneous reactions were solved using finite-rate/eddy dissipation method and heterogeneous reactions were modelled using kinetic/diffusion surface reaction model to include the reactant diffusion resistances and their behavior in a turbulent flow. The standard k-ε model was used to simulate flow of materials and energy in the turbulent regime. Performance of the reactor was improved by optimizing parameters like equivalence ratio, steam-fuel ratio, and input power to plasma torch. Zhang et al. (2013), optimized same parameters within a different numerical range and validated the predicted results with experimental runs with good agreement showcased by an error percentage of mere −4.6 %. From the gas distribution contours presented in the study it can be said that formation of CO is much faster than H_2 as high concentration of CO is found in the middle part of the reactor close to interaction point between waste and plasma. Qing et al. (2022), took inspiration for the design of downdraft plasma gasifier incorporating a circumferential injection of plasma-forming gas to increase residence time from the work of Ibrahimoglu et al. (2017), and studied the impact of three different MSW sub-components – food/paper/yard waste on syngas quality. Highest yield of H_2 of 55 mol% was observed with yard waste due to high moisture. On comparison of H_2 concentration results from Ibrahimoglu et al.'s work a deviation of +20 % is observed, potentially due to implementation of species transport model. Another contributing factor could be the inclusion of radiative heat transport in their study, where heat dissipation through radiation might limit heat available for endothermic homogeneous reactions. Although complex, as previously discussed radiative heat transfer becomes significant in large-scale plasma torches utilizing high current arcs and under these conditions radiative heat loss becomes dominant (Diab et al. 2024). Therefore, integrating radiation heat transfer model into plasma processing models is crucial for achieving more accurate results closer to real – world conditions. Models like discrete ordinates (DO), and P-1 radiation can be used to solve radiative transfer equation has they are suitable for high temperature application such as waste plasma processing and provide high fidelity responses for complex geometries (Thynell 1998).

In order to improve the efficiency of plasma processing reactors and achieve maximum conversion, uniform temperature distribution and mixing of gases must be ensured by optimizing the design and structure of the reactor. In an interesting study, Zhang et al. (2024), studied the hydrodynamics of a plasma gasification reactor with varying waste feed inlet orientations and plasma torch configurations. The initial design of oblique incident feed ports was replaced with three different orientations – tangential, diametrically opposite, and perpendicular inlets. Figure 10 shows the nephogram of plasma the gasifier with difference feed inlet orientations. From Figure 10a–c it can be observed that velocity of the particles is high near the walls when entering the reactor tangentially slows down as it moves closer to the center, thus creating a vortex allowing the particles to revolve around and experience more time inside the reactor. The temperature contours seen in Figure 10d–f show that due to the tangential feed flow, the hot gases swirling in the center are allowed to rise and a higher temperature sufficient for hetero and homogenous reactions is obtained in convergence and freeboard zones respectively. On the other hand, the particles coming in through diametrically opposite and perpendicular inlets collide in the center, thus reducing the temperature in the convergence zone and acting as a barrier for the rise of hot gases which creates undesired hot zones in the bottom part of the reactor. With this optimization it was possible to raise the maximum temperature up to 2,440 °C. Furthermore, the studies performed for the configuration of plasma torches showed that an angular injection of 23° provides slightly better temperature and velocity distribution along the reactor length.

Numerous variables come into the picture when designing a plasma reactor including geometrical parameters like reactor and plasma torch dimensions, operating conditions, special materials for refractory, electrodes, and nozzle lining and incorporating their properties (thermal conductivity, emissivity, etc.). The sheer number of permutations makes it a onerous task to explore the combinations through CFD due to computational limitations. By integrating machine learning (ML) with CFD models. ML models can efficiently learn patterns relationships between these variables and their corresponding reactor performance metrics through datasets of experimental results and CDF simulations to predict the optimum conditions for a desired outcome. In a recent study, Shi et al. (2024), explored the CFD-ML approach to optimize the geometrical configuration of a thermal plasma gasifier. For optimization, dimensions including heights, radii, and transition angles of the core reaction area and the free-board zone were considered. A dataset of 150 reactor combinations was thus created to train ML models. Gradient Booster Regression (GBR) model emerged as the most suitable model as it could incorporate the non-linear interactions between the operating parameters and analyzing the contribution of each parameter to reduce prediction errors. The predicted parameters were then refined using particle swarm optimization (PSO) and compared against CFD results an R^2 value of 0.997 and 0.954 for training and testing respectively were recorded with a low prediction error of 1.3 %. The predicted temperature in the core reaction zone (3621 K) was close to the CFD simulated value of 3668 K. Experimental validation further verified these findings. Here equivalence ratio and reaction temperature, were optimized, an ER of 0.18 provided a balance between energy efficiency and syngas calorific value, while system performance was maximized at a reaction temperature of 1700 K. Additionally, laminar plasma jet mode demonstrated superior efficiency, achieving 16.4 % higher energy efficiency and 12.4 % greater syngas calorific value compared to turbulent mode.

5.2.2 Kinetic studies

Based on the complexity of reactions and responses to be recorded kinetic studies are categorized into global, lumped and intrinsic kinetics. The most simplistic approach for pyrolysis and gasification reactions is calculating global kinetics. Here the degree of conversion of the feed as a whole into the final products over time is observed rather than calculating the rate of consumption and formation of every intermediate chemical species. This method is preferred for studying plastic waste degradation due to the varying nature of the feed. Thermogravimetric analysis-based kinetic models follow similar methodology (Bozkurt et al. 2022; Martínez-Narro et al. 2023; Perez et al. 2023), but the same experimental data cannot be used for plasma processing given the stark contrast in heating rates. Additionally, apparent kinetics are subjective to the reactor design as they are affected by the heat and mass transfer patterns inside

Table 5: Summary of CFD simulation studies carried out for waste plasma processing.

Feed	Reactor	Forming/ oxidizing gas	Dimension/ modelling approach	Study focus	Outcome	References
MSW	Plasma FB	Air/steam	2D/E-E	Parametric optimization: ER – 0.1–0.5; SFR – 0–0.8; input power – 40–100 kW	Optimal conditions – ER = 0.3; SFR = 0.5; input power = 60 kW	Ismail et al. (2019)
Coal	MW plasma DD	Air/steam	2D, 3D/E-L	Structural optimization: circumferential injection of plasma-forming gas	Increased residence time; syngas – 18.4 % (H_2), 37.2 % (CO); CGE – 55.3 %	Ibrahimoglu et al. (2017)
MSW	Plasma UD	Argon/air	2D/E-E	Temperature and mass fraction distribution in updraft gasifiers	–	Sakhraji et al. (2022)
MSW	FB-UD	Air/steam	2D/E-E	Parametric optimization: ER – 0.043–0.077; SFR – 0–0.25; DPER – 0.108–0.128	Good agreement between calculated and experimental values and optimal conditions for syngas production at ER = 0.6; SFR ≤ 0.208	Zhang et al. (2013)
Hazardous waste	Plasma UD	Air	2D, 3D/E-E	Structural optimization: Effect of varying feed inlet positions and plasma torch inclination angles	Maximum temperature increased from 2,340 °C to 2,440 °C due to tangential feed flow; better temperature distribution with angular projected torches instead of horizontal	Zhang et al. (2024)
Wood particles	HEF	Air	2D/E-L	Design optimization: effect of varying plasma outlet nozzle and feed inlet position	Improved heat distribution and residence time with increased nozzle size and reduced distance between feed inlet and plasma jet	Bastek et al. (2023)
Food/yard/ paper	FB-DD	Air	2D/E-L	Comparison of feedstock type based on syngas quality produced	Yard waste produces more H_2 (~55 mol%) due to presence of high moisture content	Qing et al. (2022)
MSW	FB-UD	Air/air, steam	0D, 2D, 3D/E-L	Parametric and structural optimization: ER – 0.1–1; SFR – 0.2–1.5; temperature – 500–2,500 K; plasma torch configuration	Required reaction volume for conversion of MSW and optimal operating conditions	Rojas-Perez et al. (2018)
MSW	FB-UD	Air	3D/E-L, GBR, PSO	Structural optimization and machine learning: optimizing reactor dimensions for a fixed design by creating a dataset within the range	Plasma gasifier designed using CFD and ML, validated with an experimental set up optimized for ER, reaction temperature and plasma jet mode	Shi et al. (2024)

the reactor. Another representation of multiple complex reactions occurring simultaneously is executed by “lumping” chemical species with similar physical, chemical, and thermodynamic properties, which progress through the reaction as a single entity. This approach is practical for complex feedstocks but the assumed homogeneity of the input stream creates scalability challenges. Moreover, ensuring robustness in such a model requires extensive pilot-scale data with various feed compositions. Supplementary Figure S5 shows the general route followed to study lumped kinetics of plastic waste. In the context of plasma processing the rate constants of conversion reactions from bulk hydrocarbon solid to wax, oil, and eventually to gas are significantly higher. As a result, it is reasonable to assume a direct conversion from solid to gas, allowing for a simplified modelling approach with fewer lumped species. Intrinsic kinetics include the fundamental molecular level kinetics that are unaffected by macrolevel extrinsic factors, meaning the resistances offered due mass and heat transfer are minimized.

Estimating kinetic parameters of thermal plasma processing of plastic waste is an onerous task due to two reasons. First, the thermal conversion process is a result of rapid pyrolysis and gasification reactions, that means a high conversion rate of the hydrocarbonaceous feed making it difficult to collect data in practical time. Second, lack of kinetic studies and data for validation and selection of model. Regarding thermal plasma pyrolysis or gasification experimental kinetic studies have been conducted for propane pyrolysis under hydrogen plasma and methane pyrolysis under microwave

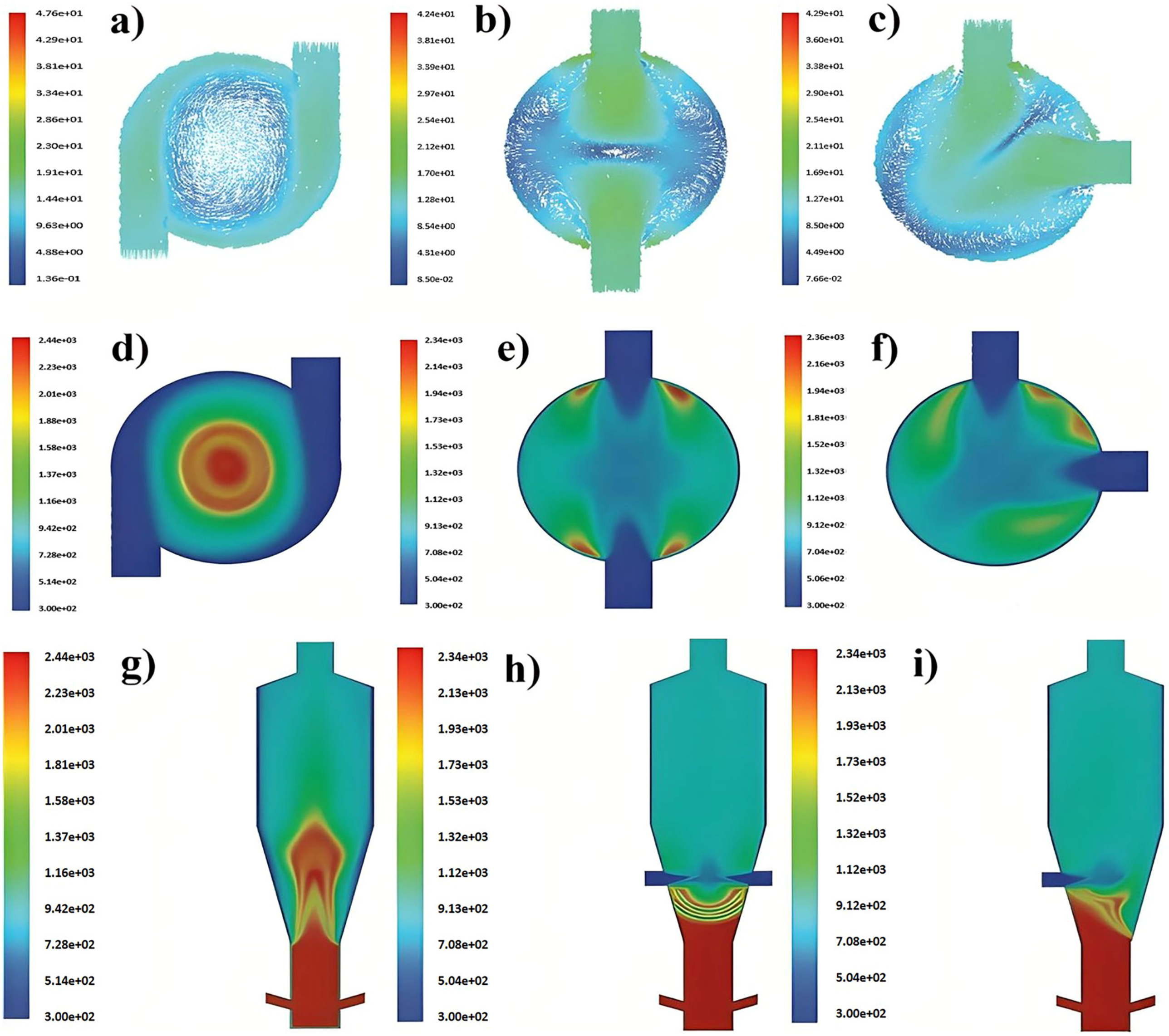

Figure 10: Comparison of the impact of tangential, diametrically opposite, and perpendicular waste feed inlet orientations on (a–c) velocity profile, (d–f) temperature distribution nephogram, (g–i) temperature distribution profile of inside the reactor, respectively. Reproduced with kind permission from, ref. (Zhang et al. 2024). Copyright 2023, Taylor and Francis.

Ar plasma by Ma et al. (2016) and Dors et al. (2014) respectively, but these works fail to provide clarity over model selection and development process.

Limited work has been published in exploring the kinetics of hydrocarbonaceous solid waste processing using plasma resulting in lack of data for validation of existing models and further development to create a set of robust equations which can accurately predict the outcome of the process. Shuangning et al. (2005), studied the plasma pyrolysis of wheat straw and corn stalk particles in a polydisperse range of 117–173 μm in a plasma heated entrained flow reactor using Ar plasma in the range of 750–950 K aiming to estimate kinetic parameters using the volumetric model, which is the most simplified technique that assumes uniform reaction rates throughout the particle volume. The first order rate of reaction is given by Equation (30), where W and W_∞ are present and final percentages of pulverized biomass.

$$\frac{\mathrm{d}W}{\mathrm{d}t} = A \cdot (W_{\infty} - W)\, e^{-E_{\mathrm{a}}/\mathrm{RT}} \tag{30}$$

The reported frequency factors and activation energies for wheat straw and corn stalk were 1,028 s^{-1}, 1,013 s^{-1} and 31.51 kJ mol^{-1}, 33.74 kJ mol^{-1} respectively. In another study Tu et al. (2009), fitted the kinetic study data for rice straw plasma pyrolysis in an integrated core model given in Equation (31):

$$\frac{\mathrm{d}M_{\mathrm{STF}}}{\mathrm{d}(t - t_{\mathrm{ST}})} = -k \cdot M_{\mathrm{STF}}^{n} \tag{31}$$

where k, is the reaction rate constant, n is the reaction order, M_{STF} denotes the residual mass fraction after reaching t_{ST}, which is the time taken to reach the set reaction temperature. The experiments were performed in a tubular reactor with a top mounted RF induced plasma torch operated between 0.35 and 0.88 kW to provide a temperature range of 740–900 K. Conversion of rice straw during plasma pyrolysis was constrained to a maximum conversion of 60 %, by operating the reactor in a differential mode to calculate the system's average reaction rate. This was done to calculate the true rate of reaction which is dependent on concentration, which drops as the reaction progresses, therefore in order to state that the rate of reaction is constant throughout the reactor, an average is calculated by maintaining low conversion values (Levenspiel 1999). Values of Arrhenius constant and activation energy were obtained as 5,759.5 s^{-1} and 74.29 kJ mol^{-1}, respectively.

These models follow the general misconception that the thermal degradation reactions occurring below 1,000 °C are kinetically controlled and thus the heat and mass transfer resistances are ignored (Mahinpey and Gomez 2016). Moreover, the values of kinetic parameters calculated through these models are subjective to the ultimate composition of the feed, this questions the strength of the model over its lack of consistency. Therefore, a model governing the rate of reaction of either C or H in the feed (as they are the largest gravimetric and molar constituent of the hydrocarbonaceous solid feed) can prove to be more robust.

For gathering preliminary experimental data for kinetic model development, operating with simpler systems such as coke, individual plastics, and coal as feed, rather than complex systems like biomass, and mixed waste can yield more accurate results as compositional variable are eliminated. Kholiavchenko et al. (2019), proposed a model to determine the kinetic constants for steam plasma gasification of wet coal. By including the thermally varying mutual diffusion coefficient of the reactant and product gases the model as presented in Equation (32) accounts for the resistance to mass transfer.

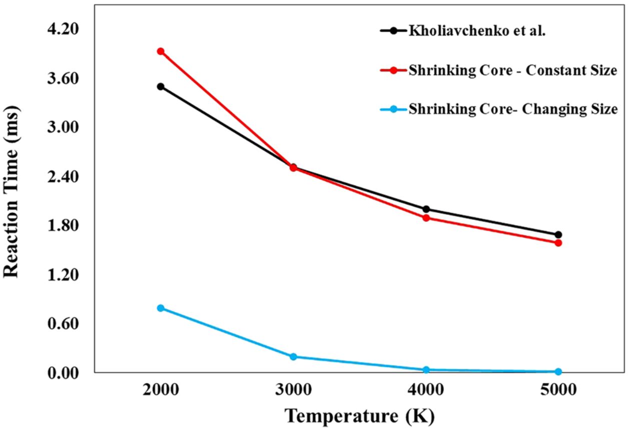

Figure 11: Comparison of total time of reaction for coal particles undergoing steam plasma gasification calculated with the proposed model (Kholiavchenko et al. 2019) and shrinking core models.

$$G_{\mathrm{C}} = \frac{\alpha_{\mathrm{d}}}{\mathrm{RT_g}}\left[\frac{N_3 \cdot p_2}{1 + N_3} + \frac{N_1 \cdot (p_1 + 0.5p_5)}{1 + N_1}\right] \tag{32}$$

where, α_{d} represents the mass transfer coefficient calculated using the Nusselt diffusion criterion, N_{i} is the dimensionless ratio of kinetic rate constant and mass transfer coefficient for the particular heterogeneous reaction, p_{i} is the partial pressure of the gaseous components, T_{g} denotes the reaction temperature, and G_{c} is the rate of gasification of carbon ($\mathrm{kmol/m^2s}$).

The assumption that the thermophysical properties of feed material remain constant throughout the heating time can be deemed appropriate for smaller particles of range 50–200 μm as considered in the study but for larger particles properties like thermal conductivity will change as the reaction progresses and products like ash and volatiles are formed. The second assumption made that the particles maintain a constant size during the heating time contradicts with general conception that a carbon based feed undergoing thermal degradation follows the mechanism of shrinking core model with changing particle size (Levenspiel 1999; Peters et al. 2012; Zhang et al. 2013). To test the theory a comparison was made in Figure 11 between the proposed model and shrinking core models for constant and changing size particles for the total time of reaction based on the data reported in the study. Equations (33–35) describe the models in discussion, here τ is the total reaction time, M_{c} is molecular mass of carbon = 12 kg/kmol, b denotes the stoichiometric coefficient = 1 in this case, D is diffusivity (the values of mutual diffusion coefficients were taken from (Massman

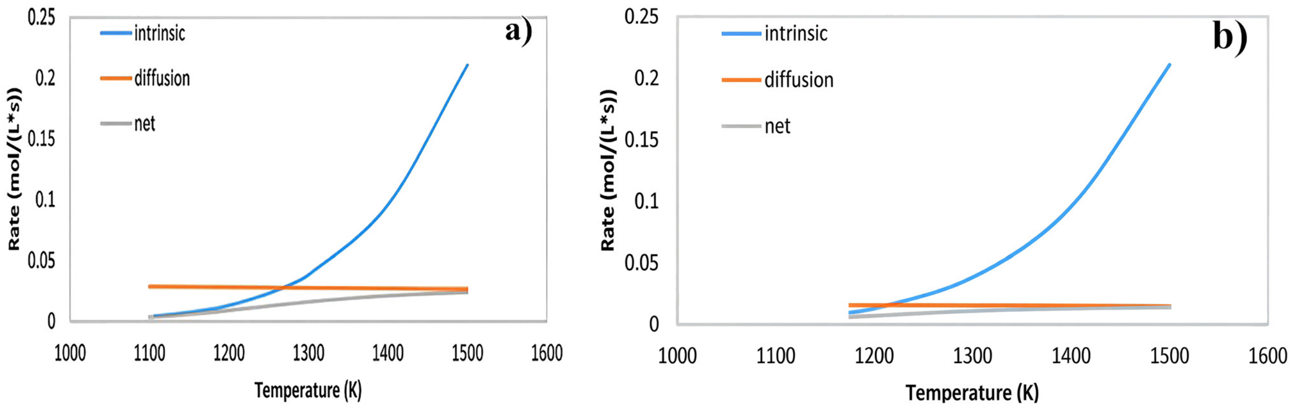

Figure 12: Comparison of reaction rates for (a) 4 in. and (b) 6 in. coke particles undergoing O_2 plasma gasification. Reproduced with kind permission from ref. (Horton et al. 2016). Copyright 2016, ACS.

1998)), C_{og} concentration of oxidizer gas, and k'' is the reaction rate constant.

$$\tau = \frac{\rho_p \cdot D_p}{2 M_c G_c} \quad \rightarrow \text{Kholiavchenko et al. 2019} \tag{33}$$

$$\tau = \frac{\rho_p \cdot D_p^2}{24 b \mathrm{D} C_{og}} + \frac{\rho_p \cdot D_p}{2 b k'' C_{og}} \quad \rightarrow \text{ Shrinking core model} \\ - \text{constant particle size} \tag{34}$$

$$\tau = \frac{\rho_p \cdot D_p}{2 b k'' C_{og}} \quad \rightarrow \text{Shrinking core model} \\ - \text{changing particle size} \tag{35}$$

For this scenario the resistance offered by the gas–solid film is neglected considering the small size (500 µm) and high gas velocity. The plot displays constant size model has good agreement with the proposed model, whereas in the changing size model diffusional resistance does not play a role as the surface is consumed during the reaction and hence shorter reaction times are obtained due to fast reactions. This comparison attempt highlights that mass transfer resistance attributed to the volatile sheath layer, however the diffusivity coefficient values must be different for volatile sheath and solid carbon unlike in this case. Therefore, is a need of an upgraded model that can account for the radially varying mass transfer resistances. However, clarity over the robustness of the model will only be obtained after experimental validation.

To determine the highest rate of reaction it is important to study the intrinsic kinetics, which are calculated by marginalizing heat and diffusional resistances, and account only the molecular level reactions. Although, it cannot be said that mass transfer resistances are eliminated, and that is why the net rate is a combination of both intrinsic and diffusion limited rate as explained in the work of (Horton et al. 2016), where the authors have defined the net rate for O_2 plasma gasification of coke as:

$$r_{\text{net}} = \frac{r_{\text{intrinsic}}}{1 + D_a} \tag{36}$$

here, $r_{\text{intrinsic}}$ is the intrinsic rate of reaction [given by Equation (37)], and D_a is the ratio of intrinsic and diffusion limited rate.

$$r_{\text{intrinsic}} = y[O_2] A_{O_2} e^{-E_{O_2}/RT} \tag{37}$$

$$D_a = \frac{r_{\text{instrinsic}}}{r_{\text{diffusion limited}}} \tag{38}$$

$$r_{\text{diffusion limited}} = k_{O_2} y [O_2] \frac{SA_p}{V_p} \tag{39}$$

y, $[O_2]$, A_{O_2}, E_{O_2}, k_{O_2}, V_p, and SA_p denote the mass fraction of oxygen in gas, concentration, pre-exponential factor, activation energy, particle volume, and surface area of the particle. For this model the surface area to volume of particle ratio is a function of time and extent of carbon conversion which accounts for the changing particle size and can be deemed apt for feed with high ash content by overcoming the shortcomings of shrinking core model to account for partially reacting core. From Figure 12 it can be inferred that diffusional limitations do become significant at temperatures higher than 1400 K. The diffusion limited regions can be shifted based on the intrinsic rate of reaction which will vary according to the plasma gas and oxidizer used.

6 Design and scale-up procedures of plasma processing reactors

The relationship between process and product scale is not always linear. Increasing the quantity of a product does not always require a proportionally larger reactor, as key factors like as mass transfer, heat transfer, mixing, and fluid flow vary with scale. Therefore, to successfully transition from lab-scale experiments to industrial-scale production, efficient reactor design is essential.

Thermal plasma processing is an emerging waste treatment technology, but the inconsistent nature of waste introduces unpredictability in outcomes and potential operational challenges. This complexity highlights the importance of carefully designing reactors, considering engineering, economic, and environmental aspects. To reduce feed complexity, studies should begin with simple feed such as individual waste plastics. The following steps outline a methodology to design and scale-up plasma processing technology for plastic waste treatment. This approach is inspired by the scale-up methodologies used in other chemical technologies, such as those presented by Joshi (2001); Yadav et al. (2017):

6.1 Step 1: understanding reactions and formulation of reaction kinetics

Understanding the key reactions occurring during plasma treatment and their mechanisms is important. The primary step is the film diffusion of plasma-forming and carrier gas followed by the vaporization of plastic waste surface, which is the thermal decomposition of macromolecules into smaller hydrocarbon vapors. This is followed by the diffusion of gases through the sheath layer to the core, the final step in the process is the gas phase reactions described in Equations (7)–(16). The kinetics of gas phase reaction are covered largely in the literature (Bustamante et al. 2005; Gómez-Barea and Leckner 2010; Jones and Lindstedt 1988; Westbrook and Dryer 1981), to identify the rate limiting steps and estimate the kinetic parameters for plasma processing the following strategy is proposed:

a) Reactor selection: a tubular semi-batch reactor in a vertical configuration is considered with a top-mounted plasma torch instead of the plasma plume immersed in the bed for better control of the reaction and observing the flow of the reaction, and figuring out hydrodynamic conditions.

b) Marginalizing heat transfer resistances: as the plasma plume impinges on the waste bed a temperature gradient develops along the length of the waste bed due to the changing thermal conductivity of the bed undergoing thermal degradation with time and the increasing loss of heat from plasma to reactor environment as the distance from plasma origin to the point of contact grows, this affects rate of reaction across the bed, therefore the feed quantity selected should be small enough to occupy a differential length (dx) that can be assumed to behave isothermally yet significant enough to produce measurable quantities of gas and solid products.

c) Marginalizing mass transfer resistances: increasing the gas velocity reduces the thickness of film boundary and therefore lowers the external mass transfer resistance. In context of waste plasma processing, the velocities of the plasma-forming gas and oxidizing/carrier gas at the film boundary can be considered approximately equal. Moreover, the velocity of plasma emitted from a DC torch can reach up to 15–40 m/s (Chau et al. 2011), making film diffusion resistance negligible. To identify intraparticle mass transfer limitations the waste particle size must be varied and the rate of reaction can be monitored by measuring the carbon moles in the gas output. An increase in reaction rate with decreasing particle size indicates mass transfer limitations, whereas a constant rate suggests a shift to the kinetically controlled regime. It can also be assumed that the reaction of other species (H, N, S, O) from the particle surface occurs in proportion to carbon.

d) Effect of concentration of oxidizing gas and carbon: the rate of reaction is concentration dependent. The concentration of oxidizing gas can vary due to the formation of gaseous products over time and the reactor's hydrodynamics. Therefore, for the assumption to stand true that a constant reaction rate exists throughout, the reactor must be operated in differential mode for small conversions limited to 50 %. Experimental runs should be conducted where the concentration of the oxidizer introduced either through the forming gas or distributed injection are varied with the help of an inert gas (mostly Ar). These experiments yield an average reaction rate corresponding to the mean oxidizer concentration in the reactor. By performing a series of such runs under a constant temperature and flow rate, a set of rate-concentration data can be generated and analyzed to derive the rate equation. Similarly, this method can be put into practice for concentration of carbon inside the reactor by varying the ultimate composition of the feed or using high melting point inerts of similar size such as powdered high alumina bricks.

e) Estimation of intrinsic kinetics: to deduce the kinetic parameters effect of temperature on degree of solid conversion must be observed. The data points can then be analyzed using the logarithmic form of the Arrhenius equation. The rate of thermal degradation increases significantly with rise in temperature given the endothermicity of the overall process. In plasma processing, however, the temperatures experienced by the feed can reach >3000 K depending on torch position and reactor hydrodynamics, under such extreme conditions the exponential term in Arrhenius equation asymptotically tends toward unity, indicating that the activation energy is much lower than the thermal energy provided therefore resulting in insignificant rise in the reaction rate despite the increment in temperature (Kholiavchenko et al. 2019).

6.2 Step 2: understanding the relationship between fluid mechanics and design objective

The primary objective of involving thermal plasma for processing plastic or solid waste, is to obtain high conversion rates, and the complete destruction of waste without generating harmful gaseous emissions and corrosive tar. The secondary goal is to utilize the produced syngas for energy recovery. To achieve these objectives, it is obvious that the feed has enough residence time in the high temperature environment, which requires establishing homogeneity inside the reactor. The velocity of gases, flow patterns, and temperature gradients in waste plasma processing reactors differ significantly from conventional pyrolysis and gasification reactors.

Insights from existing literatures and available description of commercialized technologies highlight three types of plasma reactor designs with unique flow characteristics: (i) tubular reactors with an extended freeboard zone to provide enough volume for gas phase reactions and provide better control over material flow, therefore are suitable for experimental investigations as demonstrated in several studies (Astashov et al. 2018; Hu et al. 2023; Tang et al. 2003; Zhang et al. 2013); (ii) compact plasma reaction chambers that are beneficial in establishing isothermal environment through heat circulation inside the reactor (Agon et al. 2016; Chu et al. 2023; Hlina et al. 2014; Hrabovsky et al. 2010; Hu et al. 2023; Mączka et al. 2013; Punčochář et al. 2012); (iii) plasma shaft furnaces are generally preferred for handling heterogeneous waste on a commercial scale and are subjected to large temperature gradients (Alekseenko et al. 2019; Anshakov et al. 2019a,b, 2024; Byun et al. 2010, 2012). The flow of the materials is also governed by the bed arrangement inside the reactor. Tang et al. (2013) in their review discuss in detail about various bed arrangements in waste plasma processing reactors, comparing their ease of operation and effects on degree of waste conversion. Additionally, the position of plasma torch inside the reactor plays a crucial role in determining the flow regime. Reactors with a top-mounted plasma torch facilitate complete waste conversion by allowing the gas, formed during the breakdown of solid materials, to re-interact with the high-temperature plasma before exiting the reactor (Hlina et al. 2014; Hrabovsky et al. 2010; Tang and Huang 2007; Tang et al. 2003). However, the plasma loses a significant amount of heat through radiation due to the distance between feed and plasma origin point, and results in temperature drop from 5,000 – 10,000 K to 2000 K. Another widely adapted configuration is immersing the plasma jet inside the waste bed (Mączka et al. 2013; Punčochář et al. 2012), here the waste feed experiences extremely high temperatures resulting in a higher rate of reaction can, However, the high velocity of the thermal plasma can entrain unconverted waste in the upper layers, reducing overall efficiency. To overcome this issue Byun et al. (2010) designed plasma chambers with recirculation zones. In their design, the plasma torch is aligned at a 30° angle, leveraging centrifugal force to enhance heat distribution and ensure sufficient heating of the feed, thereby minimizing waste entrainment and improving conversion efficiency.

Furthermore, visualizing the movement of particles and gas flow inside the reactor system can be done with CFD modelling studies and through empirical methods such as particle image velocimetry, or high-speed imaging. Visualization of plasma arc generated through DC and AC torches can also be done with the help of charge-coupled device (CCD) cameras working at shutter speeds of up to 1/8,000 s (Rutberg et al. 2013). Videography of plasma arcs can help in determining the arc velocity to calculate residence times and arc diameter, which can aid in estimating heat distribution and accordingly optimize the reactor.

6.3 Step 3: optimization of parameters

Optimization of plasma waste processing involves managing multiple variables, as shown in Figure 13. Independent factors such as feed rate, gas flow rate, torch power, and reactor geometry influence flow dynamics and

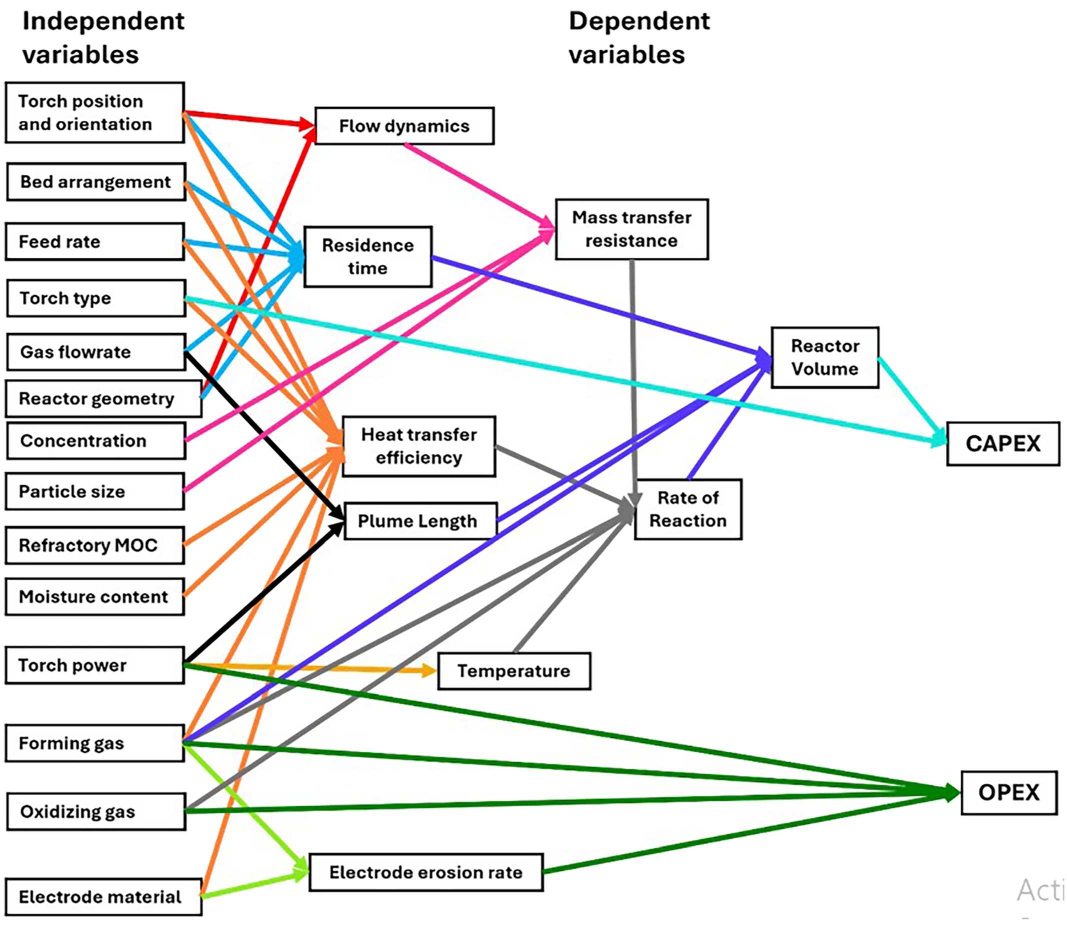

Figure 13: Mind-map illustrating interdependencies between parameters for optimization of waste plasma processing technology.

residence time, which in turn affect mass and heat transfer, and reaction rates. Additionally, adjusting the torch position and bed arrangement must be done as well to optimize flow dynamics, and factors like particle size and moisture content must be controlled to improve heat transfer efficiency.

Dependent variables like CAPEX and OPEX are shaped by reactor volume and electrode erosion, which can be minimized by selecting suitable forming gases and electrode materials. High-quality syngas output requires careful tuning of oxidizing and forming gas compositions based on feed characteristics. Advanced tools like CFD and real-time monitoring can support system optimization, improving performance, reducing costs, and enhancing environmental sustainability.

6.4 Step 4: implementation

Before scaling up a plasma processing plant, validating the design through pilot tests is essential to confirm assumptions. Key components like plasma torches and reactors must be tested under full load. Large-scale operations also demand advanced process control and automation systems that can adjust plasma power, gas flow rates, and feed rates in real-time, ensuring stable performance and safety. Automations like, automatic shutdowns and gas venting during abnormal conditions, and helps manage fluctuations in feedstock quality (Sharma 2017). Safety remains a priority due to the high temperatures and pressures involved, so installing pressure relief valves, explosion-proof designs, and fire suppression systems is essential (Hall 2012). Furthermore, environmental controls must be in place, including emissions control systems like scrubbers and bag filters, to meet regulatory standards. Additionally, securing a reliable feedstock supply chain is crucial for continuous operation, requiring pre-processing facilities and careful logistics for sourcing, transporting, and storing plastic waste. Finally, waste management should focus on efficient slag disposal, syngas utilization, and profitability assessment through techno-economic analysis (TEA), discussed further in the next section.

Table 6: Comparison of economic studies on plasma gasification (values in $ millions).

Plant capacity (TPD)	**10**	**70**	**100**	**300**	**500**	**2000**
Year	2012	2024	2012	2010	2024	2015
Working days	330	300	330	330	350	330
Region	Cheongsong, South Korea	China	Cheongsong, South Korea	Iowa, USA	–	Abu Dhabi, UAE
Capital cost	**3.9**	**25.57**	**24.8**	**107.2**	**125.5**	**601.7**
Plant fabrication	–	–	–	48.3	35.4	162
Plasma torch	–	–	–	27.4	47.1	–
Energy recovery unit	–	–	–	17.7	16.07	145.64
Others	–	–	–	13.8	26.93	–
Annual operating cost	**0.99**	**2.557**	**3.34**	**8.9**	**9.83**	**22.78**
Electricity (GWh/year)	–	–	15.84	–	–	–
Maintenance	–	2.557	–	3.1	–	15.36
Disposal	–	–	–	0.57	–	–
Other	0.77	–	2.51	1.2	–	–
Annual revenue	**–**	**15.37**	**6.2**	**–**	**3.2**	**112.508**
Electricity sold (GWh/year)	–	59.13	23.8	–	–	993.4
Net electricity sales	–	5.706	2.6		–	69.5
Slag sale	–	0.00114	–	–	–	0.108
Tipping fee ($/ton)	–	466.2	110	–	–	65
Waste treatment sales	–	9.67	3.6	–	–	42.9
References	Byun et al. (2012)	Wang et al. (2025)	Byun et al. (2012)	Clark and Rogoff (2010)	Anilkumar et al. (2024)	Mazzoni and Janajreh (2017)

7 Techno-economic analysis

Studying the economic feasibility of a new technology on large scale is crucial for its acceptance and implementation. From a practical standpoint, the installation of energy intensive waste processing facilities is significantly influenced by the region. Factors like government policies, tipping fee, waste generation magnitude to population ratio, and availability of space vary globally and raises the discussion for profitability of waste processing compared to landfilling. Landfilling remains cost-effective in spacious, low-population areas, like USA where the tipping fee is $56.8/ton MSW (Statista 2025). On the other hand, waste processing facilities can be fruitful where land is scarce, such as UK, Belgium, and Japan where a tipping fee of $103, $110/ton, and $200–300/ton of MSW disposal is levied, respectively (Cyranoski 2006; European Environment Agency 2023, Green Bank Waste Solutions 2024). The economics may also fit right for regions with extremely high waste generation rate for example China, where 30 MMT/annum plastic waste is generated with a landfilling cost of $175/ton (Jiang et al. 2024).

The economic assessment of thermal plasma waste processing remains challenging due to its low technology readiness level, which limits cost optimization opportunities. A significant portion of the total capital investment (TCI) comes from the plasma gasifier unit (Munir et al. 2019). The plasma torch, absent in conventional thermochemical techniques, itself is a major contributor due to the requirement of specialized electrode and nozzle materials to resist high temperature erosion, and proprietary manufacturing technology (Clark and Rogoff 2010; Venkatramani 2002 estimated the cost of plasma arc to be $27.4 million which is roughly 30 % of the TCI for a 300 TPD plant in Iowa, USA. Other adders to the TCI include the combined cycle system (comprised of gas turbine, heat recovery steam generator, and a steam turbine), and gas cleaning unit (Kwon and Im 2024). A comparison of capital costs estimation from several plasma gasification economic studies has been provided in Table 6. Economic studies from various regions have been presented in the table therefore to update and accommodate cost variability, the chemical engineering plant cost index and domestic factor for plasma systems can be found elsewhere Aich et al. (2024). From the table it is clear that very less information is available about the pricing of plasma torches and plasma gasifiers due to the varying scales of these studies. Moreover, there is a need of standardization in the field to estimate at least the theoretical costing and it can be achieved with investigating kinetics of the system. Anilkumar et al. (2024), estimated a cost of $ 47.1 million for plasma torches powering a 500 TPD MSW plasma gasification plant. The cost of installation of energy recovery units is approximately 15–25 % of the plasma gasification facility, these values closely side with those reported for the case of conventional gasification plants. Integration of plasma gasification with energy recovery systems play a key role in making the process beneficial and self-sufficient for the most part by recovering operating costs.

Detailed information over the operating costs of plasma processing plants is very rare and that available in literature does not provide breakdown of the overall values. The opex numbers are considered similar to those of conventional gasification studies. However, this analogy fails as the plasma plants consume the most expensive form of energy, electricity, in large amounts as their main source of heat. Byun et al. (2012), based on the data from their 10 TPD plasma gasification plant calculated that 480 kWh/ton of electricity will be required for a 100 TPD unit. Ducharme (2010), compared the economics of existing plasma gasification facilities and concluded that technologies that involve plasma gasification as the primary waste treatment technique require 24–40 % less operating cost per ton of waste compared to technologies that use plasma as a secondary treatment, to clean raw syngas produced through conventional gasification. This is due to the higher efficiency of plasma processing, and lower energy consumption as it is a single step conversion. Furthermore, the maintenance charges are heavily influenced by the electrode erosion rate, in non-transferred torches a small defect in the anode ring requires the torch to be immediately replaced. Recycling old torch parts thus becomes important to lower operational costs. Lifetime of electrodes can be increased by using inerts such as Ar in mixture with the oxidizing forming gas. Moreover, the opex of the process can further be lowered by pre-processing the feed, as in size reduction and moisture removal to work with higher kinetic rate constants as discussed before (Aliferov et al. 2016; Anshakov et al. 2019a,b).

Revenue generation in plasma gasification occurs through multiple streams, majorly waste treatment tipping fee, and supported by power or syngas sales, slag sales, and also renewable energy credits. Tipping fees as discussed, vary widely with the location, capacity of the plant, and the type of waste treated. The tipping fee for treating biomedical waste in a plasma gasification plant with a capacity of 70 TPD is $466.2 per ton (Wang et al. 2025).

Electricity sales are the second most significant revenue source. Integrated plasma gasification combined cycle (IPGCC) plants produce electricity using gas and steam turbine for self-sustenance and surplus sales. Simulational study for a 2,000 TPD plant displays the potential to sell 993.4 GWh of electricity annually, generating $ 69.5 million in revenue (Mazzoni 2017). Slag sales and renewable energy credits are less reliable contributors and only makes sense to be accounted at the industrial scale. Hence, with a diverse revenue model plasma waste processing shows great potential as a feasible technology for waste management and renewable energy production.

8 Commercialization attempts across the globe

The development of high-temperature thermal plasma followed the advancements in plasma torch technology, which enabled its widespread use in the metallurgical industry as a heat source for metal melting and extraction in the 1970s and 80s (Boulos et al. 2016b). Companies such as Westinghouse (now owned by Harvest International New Energy), Tetronics, Europlasma, and Phoenix Solutions developed proprietary plasma torch technologies, making them the pioneers in commercializing plasma processing for waste management. The successes and challenges of these commercialization attempts are discussed in Sections 8.1 and 8.2.

8.1 Past and present installations

The primary drivers for adopting plasma technology in the waste management sector are regulatory pressures for mitigation of hazardous waste, reduction of waste volume, minimization of harmful emissions without the need of extensive sorting and cleaning of the waste, and to some part economic factors such as gate fee. These are also the reasons why plasma gasification saw widespread commercialization globally compared to plasma pyrolysis and incineration. In 1990 the Westinghouse Plasma Corporation (WPC) commissioned its first 48 TPD plasma gasification testing facility in Madison, USA where they tested over 100 feedstocks and for their potential to produce syngas. Based on their water cooled non-transferred DC plasma torch technology, WPC, as a subsidiary of the Alter NRG group established numerous waste to energy plants across Asia with the most recent ones in Wuhan and Shanghai, China. The European market share is significantly captured by companies like Europlasma and

Tetronics. Europlasma has setup plasma vitrification and gasification plants with Inertam and CHO-Power respectively in Morcenx, France. Tetronics, based in the UK, has commercialized transferred DC arc graphite-electrode technology in collaboration with Advanced Plasma Power, establishing syngas production plants utilizing waste plastics and biomass. As previously mentioned, initially plasma processing facilities were primarily focused on melting hazardous wastes, including medical waste, polychlorinated biphenyls, radon-based paints, nuclear waste, and asbestos. InEnTec®'s plasma enhanced melting (PEM) technology was instrumental in addressing these challenges throughout the 1990s (Achinas 2019). However, over time, a clear shift has occurred in the strategic intent of plasma technology deployment. Emerging installations are increasingly focused not only on safe disposal but also on resource recovery, particularly hydrogen and syngas production for energy or chemical synthesis. This trend is driven by technological maturation and the growing economic viability of synthetic fuels. In 2012, South Korea-based start-up Green Science Platech (GS Platech) commissioned a 10 TPD MSW processing plant in Cheongsong-gun city, capable of producing 20 Nm^3/hr of H_2 (Byun et al. 2012; Sesotyo et al. 2019). In 2021, GS Platech also launched the world's first microwave plasma-based gasification plant in Taebaek, South Korea, which produces 3 MW of electric power annually from plastic waste and wooden chips (Pulse 2024). Another emerging start-up, SGH2, has established a 3,800 tpy H_2 plant using its proprietary Solena Plasma Enhanced Gasification (SPEG) technology to process waste biomass (SGH2 Energy 2024). A summary of other commercialization attempts is provided in Table 7.

8.2 Challenges with commercialization

The four leading stumbling blocks for large scale commercialization of plasma processing of waste are (i) regulatory frameworks, (ii) market agreement and acceptance, (iii) technological maturity, and (iv) social acceptance. Regulations and societal aspects are linked and present the most significant challenge in establishing a plasma processing plant for waste treatment. The construction of plasma gasification or pyrolysis facilities, which include thermal reactors operating at extremely high temperatures and high-caloric hazardous waste storage units, often raises significant public concerns about potential harmful air emissions, fire risks, and toxic chemical leachate; such facilities have faced cancellation in the past due to economic issues, public mistrust, and safety concerns. Such concerns necessitate stringent regulations from institutions like the World Health Organization (WHO) and Central Pollution Control Board (CPCB) to ensure the safe operation of plasma technology (Das et al. 2020). An assessment carried out by Sampathraju and Mansuri 2019 highlighted that air pollutants from plasma disposal plant for biomedical waste were well below than conventional incineration and commit to the limits set by CPCB. Furthermore, ensuring the safety and stability of plasma plants to prevent accidents becomes the responsibility of local authorities who must conduct rigorous safety and environmental audits, and facilitate community feedback that can also help in advocacy of the technology to set up more plants. Additionally, regulatory requirements for operating permits for energy-intensive plants and agreements for the treatment of hazardous wastes are essential for plasma processing companies. These regulations not only ensure compliance with environmental standards but also impact the financial viability and profitability of the business. Thus, navigating the regulatory landscape and addressing societal concerns are fundamental for the successful implementation and growth of plasma processing technology in waste management.

Challenges in commercialization also occur when complete technology readiness is not achieved (Munir et al. 2019). Technical failures in plasma gasification and pyrolysis plants often arise due to aggressive scale-ups, when technologies that are only at a demonstration level are scaled up to 10 folds it leads to problems such as formation of cold spots. This was the situation faced during operation of the Hitachi Metals plasma gasification plant in Utashinai, Japan where the large bottom diameter led to uneven heat distribution resulting in lower conversion, this ultimately led to entrainment of particulates with the produced syn-gas and attacking the refractory lining. This case highlights the importance of prudential reactor design in terms of ensuring proper heat transfer, residence time calculations, and high temperature resistive refractory linings. Similarly, the Teesside, England plasma gasification project, which aimed to construct two 50 MW plants, was abandoned due to the technology's failure at scale. Besides technological issues, which are solvable, strategic planning for raw material supply is crucial. The closure of the Hitachi plasma plant in Eco-valley, Utashinai, was partly due to increased recycling practices that led to a shortage of MSW feed, highlighting the need for agreements with local authorities to secure a consistent feedstock supply (Hrabovsky et al. 2022.). This makes the location of the plant an important element in the successful establishment of plasma gasification plants for waste treatment. Having a plasma gasification plant established in a location with high waste generation capacity to available landmass ratio will be beneficial as it ensures consistent feed supply. Alternatively, portable or on-site plasma processing units are being explored as flexible

Table 7: Globally commissioned commercial and pilot plasma waste processing plant.

Owner	City	Country	Technology supplier	Capacity (tpd)	Feedstock	Output	Year
Nufarm Limited	North Laverton, Victoria	Australia	SRL Plasma – PLASCON	0.8	Chlorophenols, phenoxies, toluene, dioxins/furans		1995
BCD Technologies			SRL Plasma – PLASCON	1	Concentrated polychlorinated biphenyl (PCB) waste		1997
PyroGenesis	Montreal	Canada	PyroGenesis	0.5–2.5	Mixed waste		2002
Plasco Energy Group	Ottawa		Plasco Energy Group	85	MSW	Power	2007
Wuhan Kaidi	Wuhan, Hubei	China	Alter NRG	150	Biomass	Syngas to Diesel (Fischer Tropsch)	2012
Abada Plasma Technology Holdings	Shanghai		PEAT International	1.2	Medical waste, oil refinery sludge		2013
GTS Energy	Shanghai		Alter NRG	30	Medical waste, incinerator fly ash	Slag	2014
CHO-Morcenx	Morcenx	France	Europlasma	140–150	Cardboard, wood, paper, tissues	12 MW	2012
SMS Envocare	Nagpur	India	Alter NRG	68	Hazardous waste	Power	2008
SMS Envocare	Pune		Alter NRG	68	Hazardous waste	Power	2009
EnvironmentalEnergy Resources Ltd		Israel	EnvironmentalEnergy Resources Ltd	20	MSW	Plasma Rocks	
Hitachi Metals, Hitachi	Yoshi	Japan	Alter NRG	151	MSW		1999
Hitachi Metals, Hitachi	Mihama-Mikata		Alter NRG	24	MSW, WW sludge	Syngas + 1.5 TPD slag	2002
Fuji Kaihatsu Ltd.	Iizuka		InEnTec	10	Electronic scrap	Gold + copper	2002
Hitachi Metals	Utashinai, Hokkaido		Alter NRG	220	MSW, ASR	7.9 MWh power and return-4.3 MWh to grid	2003
Kawasaki	Okinawa		InEnTec		PCB oil and PCB-contaminated materials		2003
Kawasaki Plant Systems	Harima		InEnTec		Asbestos		
Boeing Company/Bio-Pure Systems	Kuala Lumpur	Malaysia	InEnTec				
Dunarea SA	Brasov	Romania	Bellwether RG	240	Calorific waste	Power, heat	2008
GS Plastech	Cheongsong	South Korea	GS Plastech	10	MSW	50 kW	2008
Taebaek Cheoram Power Plant	Taebaek		Green Science		Wood chips + plastic waste	3 MW	2021
National Cheng Kung University	Tainan	Taiwan	PEAT International	5	Waste and toxic waste such as incinerator fly ash, medical waste, inorganic sludges		2005
Global Plasma Technology Limited	Kuan Yin (Taipei)		InEnTec	24 + 4	MSW + sewage sludge		
NG, Stonehouse, PR, CNG Services	Wiltshire	United Kingdom	Advanced Plasma Power	300	Waste, biomass	Syngas, power	2008
	Energy Park Peterborough		Advanced Plasma Power		Mixed waste	Power	2014
NG, Advanced Plasma Power, PE	Swindon, Wiltshire		Advanced Plasma Power	22	RDF	bioSNG	2017
Alter NRG	Madison, Pennsylvania	USA	Alter NRG	48	Multiple feed testing (100+)	Syngas	1990
InEnTec LLC	Richland		InEnTec	4	Hazardous waste		1996
InEnTec LLC	Richland		InEnTec		Hazardous and nuclear waste, TSCA and PCB waste		1999

Table 7: (continued)

Owner	City	Country	Technology supplier	Capacity (tpd)	Feedstock	Output	Year
Allied Technology Group, Inc.	Richland		InEnTec		Mixed hazardous and radioactive wastes		1999
Asia Pacific Environmental Technologies	Kapolei		InEnTec		Medical waste	Power	2001
	US Navy		PyroGenesis	7	Shipboard wastes		2004
Air Force Special Operations Command	Hurlburt Field		PyroGenesis	10.5	MSW, hazardous wastes		2011
	Lorton, Virginia		PEAT International	7	Defense department waste, medical waste		
InEnTec Columbia Ridge LLC	Arlington		InEnTec		MSW	Syngas, H_2	
Dow Corning Corp.	Midland, Michigan		InEnTec		Industrial by-products		

solutions to address the dual challenges of waste accessibility and the limited processing capacities often associated with large-scale, centralized plasma facilities.

9 Conclusions

The plastic waste problem affects nearly every industry and environment, mixing with other waste streams and creating complex combinations. Current thermochemical recycling methods face several operational and environmental challenges in dealing with these contaminated, mixed, or chlorinated plastics. An inflection point in the treatment of complex solid wastes is the thermal plasma technology, which represents more than just “hotter versions” of conventional thermal processes. Thermal plasma tackles three key challenges in waste management simultaneously (i) heterogeneity of waste, (ii) maximum contaminant destruction, and (iii) process intensification by compact reactor designs and rapid kinetics. However, scaling this technology demands deeper investigation into thermal plasma-specific kinetics, heat/mass transfer, and integrated system design, areas where fundamental engineering insights remain sparse. This review has systematically evaluated these challenges, paving the way for actionable solutions to bridge lab-scale innovation and industrial deployment. To realize the potential of this technology, the field must move beyond the assumptions carried over from combustion and conventional thermochemical research. As global plastic production continues to rise, such innovations are no longer optional, they are imperative.

Current understanding of thermal plasma waste processing faces critical limitations in both fundamental mechanisms and computational modeling approaches. While mathematical models have been developed to study various aspects including particle heating times, chemical reaction energies, and plasma gas properties – they universally struggle to capture plasma-specific phenomena. The extremely short lifespans of charged species and radicals make their interactions with feedstock difficult to measure, creating a knowledge gap in non-thermal reaction pathways and accounting for mass transfer limitations. Existing heat transfer models often inherit inappropriate assumptions from entrained-bed configurations, particularly regarding uniform particle heating and negligible radiative transfer, despite evidence that radiation becomes dominant in high-power systems.

Recent computational studies have made significantly addressed these gaps through innovative approaches. Advanced radiation models now enable more accurate simulation of heat dissipation in large-scale systems, though their complexity limits widespread adoption. Cutting-edge CFD work has revealed how reactor geometry profoundly affects performance, with optimized feed inlet configurations and torch angles demonstrating measurable improvements in temperature distribution and flow patterns. However, these models still cannot simultaneously resolve particle-scale phenomena and system-scale hydrodynamics, forcing compromises between accuracy and computational feasibility. The integration of ML with CFD presents a promising path forward, enabling efficient exploration of the vast parameter space in reactor design. These hybrid approaches can identify optimal configurations by learning patterns from existing data, though they currently suffer from limited training sets that lack plasma-specific kinetic information.

Key research directions include:

(i) Developing multiphysics models that couple radiation, electromagnetics, and discrete phase behavior.

(ii) Carrying out experimental studies for plasma-specific kinetics and charged species interactions to better validate modelling results.

Despite plasma technology's advantages in waste conversion and emission control, its commercialization faces intertwined technical and societal barriers. Scaling reactors while maintaining temperature uniformity remains challenging, as evidenced by past plant failures. Concurrently, public skepticism and evolving regulations create additional hurdles for deployment, even as studies confirm superior environmental performance versus conventional methods. These challenges demand solutions that address both engineering fundamentals and stakeholder concerns.

To address these barriers, a systematic scale-up methodology is proposed:

(i) Fundamental studies: establish intrinsic reaction kinetics using controlled experiments that minimize heat/mass transfer resistances, enabling accurate modeling of plasma-specific pathways.
(ii) Reactor optimization: combine CFD and machine learning to optimize geometry, torch positioning, and flow dynamics while accounting for radiative heat transfer at scale.
(iii) Pilot validation: test designs under real-world conditions, integrating automation for process stability and safety.
(iv) Stakeholder engagement: collaborate with regulators and communities to demonstrate safety and environmental benefits.

By bridging fundamental research with engineered solutions, plasma technology can transition from promising innovation to viable waste management alternative. The path forward demands interdisciplinary efforts – advancing reactor designs while fostering regulatory and public confidence, to unlock its potential for sustainable plastic waste management.

Acknowledgments: The authors gratefully acknowledge the financial support from the J. B. Joshi Research Foundation, to carry out this work.
Research ethics: Not applicable.
Informed consent: Not applicable.
Author contributions: All the authors have accepted responsibility for the entire content of this submitted manuscript and approved submission. KS: data curation, methodology, writing - editing original draft. MDY: conceptualization, methodology, supervision, editing. AS: reviewing. SB: reviewing. SG: reviewing. JBJ: supervision, funding, administration.
Use of Large Language Models, AI and Machine Learning Tools: Not applicable.
Conflict of interest: The authors declare that they have no conflict of interest.
Research funding: Financial support was received from the J. B. Joshi Research Foundation.
Data availability: Not applicable.

References

Abedsoltan, H. (2023). A focused review on recycling and hydrolysis techniques of polyethylene terephthalate. *Polym. Eng. Sci.* 63: 2651–2674.

Achinas, S. (2019). An overview of the technological applicability of plasma gasification process. In: Singh, P., Singh, R.P., and Srivastava, V. (Eds.). *Contemporary environmental issues and challenges in era of climate change*. Springer, Singapore, pp. 261–275.

Agon, N., Hrabovský, M., Chumak, O., Hlína, M., Kopecký, V., Mašláni, A., Bosmans, A., Helsen, L., Skoblja, S., Van Oost, G., et al. (2016). Plasma gasification of refuse derived fuel in a single-stage system using different gasifying agents. *Waste Manag.* 47: 246–255.

Agun, L., Ahmad, N., Redzuan, N.H., Misnal, M.F.I., and Zainal, M.N.F. (2022). Plasma technology in waste-to-energy valorization: fundamentals, current status, and future directions. In: Jacob-Lopes, E., Queiroz Zepka, L., and Costa Deprá, M. (Eds.). *Handbook of waste biorefinery*. Springer, Cham, pp. 813–830.

Aich, W., Hammoodi, K.A., Mostafa, L., Saraswat, M., Shawabkeh, A., Jasim, D.J., Ben Said, L., El-Shafay, A.S., and Mahdavi, A. (2024). Techno-economic and life cycle analysis of two different hydrogen production processes from excavated waste under plasma gasification. *Process Saf. Environ. Prot.* 184: 1158–1176.

Al-Ghouti, M.A., Khan, M., Nasser, M.S., Al-Saad, K., and Heng, O.E. (2021). Recent advances and applications of municipal solid wastes bottom and fly ashes: insights into sustainable management and conservation of resources. *Environ. Technol. Innov.* 21: 101267.

Alekseenko, S.V., Anshakov, A.S., Domarov, P.V., and Faleev, V.A. (2019). Experimental plasma setup for gasification of organic waste with their discrete supply into gasifier. *Thermophys. Aeromech.* 26: 939–943.

Aliferov, A.I., Anshakov, A.S., Sinitsyn, V.A., Domarov, P.V., and Danilenko, A.A. (2016). Modeling ohmic heating in the drying zone of the plasma shaft electric furnace, when recycling the technogenic waste. *J. Phys. Conf. Ser.* 754: 112002.

Amirahmadi, H., FarshiFasih, H., Saviz, S., and Nobakhti, M.H. (2024). Experimental and modeling study of medical waste based on plasma gasification. *Waste Manag.* 186: 198–204.

Anilkumar, R., Vinayak, A.K., Kiran, B., and Gurumoorthy, A.V.P. (2024). Study of municipal solid waste treatment using plasma gasification by application of Aspen Plus. *Chem. Prod. Process. Model.* 19: 901–915.

Anis, S. and Zainal, Z.A. (2011). Tar reduction in biomass producer gas via mechanical, catalytic and thermal methods: a review. *Renew. Sustain. Energy Rev.* 15: 2355–2377.

Anshakov, A.S., Aliferov, A.I., and Domarov, P.V. (2019a). Features plasma gasification of organic waste. *IOP Conf. Ser. Mater. Sci. Eng.* 560: 012057.

Anshakov, A.S., Domarov, P.V., Perepechko, L.N., and Faleev, V.A. (2019b). Studying plasma gasification of solid municipal waste. *J. Phys. Conf. Ser.*, https://doi.org/10.1088/1742-6596/1261/1/012003.

Anshakov, A.S., Domarov, P.V., and Faleev, V.A. (2024). Studying the technology for destroying infected waste in low-temperature plasma. *Thermophys. Aeromech.* 31: 185–188.

Astashov, A.G., Samokhin, A.V., Alekseev, N.V., Litvinova, I.S., and Tsvetkov, Y.V. (2018). Heat and mass transfer in confined jet plasma reactor with peripheral vortex flow. *J. Phys. Conf. Ser.* 1134: 012004.

Bastek, S., Wilhelm, S., Fahmy, M., Fendt, S., and Spliethoff, H. (2023). Optimization of a horizontal entrained flow plasma gasification test rig through CFD-simulation. In: *36th Int. Conf. Efficiency, Cost, Optim., Simul., Environ. Impact Energy Syst. (ECOS 2023)*, pp. 512–523.

Bei, J., Xu, X., Zhan, M., Li, X., Jiao, W., Khachatryan, L., and Wu, A. (2022). Revealing the mechanism of dioxin formation from municipal solid waste gasification in a reducing atmosphere. *Environ. Sci. Technol.* 56: 14539–14549.

Benedetto, J.A., Binetti Basterrechea, F.E., Neira, G.F., Lago, L.A., Prado, D.C., Williams, C., Soroush, M., Pullao, J.A., Benedetto, F.E., Franco, G., et al. (2024). Plasma gasification of a simulated low-level radioactive waste: co, Cs, Sr, and Ce retention efficiency. *Processes* 12: 1919.

Bhatt, K.P., Patel, S., Upadhyay, D.S., and Patel, R.N. (2022). A critical review on solid waste treatment using plasma pyrolysis technology. *Chem. Eng. Process. - Process Intensif.* 177: 108989.

Bhatt, K.P., Patel, S., Upadhyay, D.S., and Patel, R.N. (2024). Production of hydrogen-rich fuel gas from waste plastics using continuous plasma pyrolysis reactor. *J. Environ. Manag.* 356: 120446.

Boulos, M.I., Fauchais, P.L., and Pfender, E. (2016a). *Handbook of thermal plasmas*. Springer, Cham.

Boulos, M.I., Fauchais, P.L., and Pfender, E. (2016b). The plasma state. In: Boulos, M.I., Fauchais, P.L., and Pfender, E. (Eds.). *Handbook of thermal plasmas*. Springer, Cham, pp. 1–53.

Bozkurt, O.D., Okonsky, S.T., Alexopoulos, K., and Toraman, H.E. (2022). Catalytic conversion of SPW and products upgrading. *Adv. Chem. Eng.* 60: 117–168.

Buekens, A. and Zhou, X. (2014). Recycling plastics from automotive shredder residues: a review. *J. Mater. Cycles Waste Manag.* 16: 398–414.

Bustamante, F., Enick, R.M., Killmeyer, R.P., Howard, B.H., Rothenberger, K.S., Cugini, A.V., Morreale, B.D., and Ciocco, M.V. (2005). Uncatalyzed and wall-catalyzed forward water–gas shift reaction kinetics. *AIChE J.* 51: 1440–1454.

Byun, Y., Cho, M., Hwang, S.M., and Chung, J. (2012). Thermal plasma gasification of municipal solid waste (MSW). In: *Gasification for practical applications*. InTech.

Byun, Y., Namkung, W., Cho, M., Chung, J.W., Kim, Y.S., Lee, J.H., Lee, C.R., and Hwang, S.M. (2010). Demonstration of thermal plasma gasification/vitrification for municipal solid waste treatment. *Environ. Sci. Technol.* 44: 6680–6684.

Cai, X. and Du, C. (2021). Thermal plasma treatment of medical waste. *Plasma Chem. Plasma Process.* 41: 1–46.

Cerqueira, N., Vandensteendam, C., and Baronnet, J.M. (2006). Heavy metals behavior during thermal plasma vitrification of incineration residues. *AIP Conf. Proc.* 812: 120–127.

Chu, C., Wang, P., Boré, A., Ma, W., Chen, G., and Wang, P. (2023). Thermal plasma co-gasification of polyvinylchloride and biomass mixtures under steam atmospheres: gasification characteristics and chlorine release behavior. *Energy* 262: 125385.

Chau, S.W., Lu, S.Y., and Wang, P.J. (2011). Modeling of axis-symmetric steam plasma flow in a non-transferred torch. *Comput. Phys. Commun.* 182: 152–154.

Chen, S., Liu, Z., and Zhao, X. (2025). Thermodynamic modeling of thorium migration behavior in Th-doped GTA tungsten electrode. *Energy* 314: 134277.

Choudhury, M., Sahoo, S., Samanta, P., Tiwari, A., Tiwari, A., Chadha, U., Bhardwaj, P., Nalluri, A., Eticha, T.K., and Chakravorty, A. (2022). COVID-19: an accelerator for global plastic consumption and its implications. *J. Environ. Public Health* 2022: 1066350.

Chu, J.P., Hwang, I.J., Tzeng, C.C., Kuo, Y.Y., and Yu, Y.J. (1998). Characterization of vitrified slag from mixed medical waste surrogates treated by a thermal plasma system. *J. Hazard. Mater.* 58: 179–194.

Clark, B.J. and Rogoff, M.J. (2010). Economic feasibility of a plasma arc gasification plant, city of Marion. In: *IOWA. 18th Annu. North Am. Waste-to-Energy Conf., NAWTEC18*, pp. 121–130.

Cortazar, M., Santamaria, L., Lopez, G., Alvarez, J., Zhang, L., Wang, R., Bi, X., and Olazar, M. (2023). A comprehensive review of primary strategies for tar removal in biomass gasification. *Energy Convers. Manag.* 276: 116496.

Cottom, J.W., Cook, E., and Velis, C.A. (2024). A local-to-global emissions inventory of macroplastic pollution. *Nature* 633: 101–108.

Cvetinović, D., Erić, A., Mladenović, M., Buha-Marković, J., and Janković, B. (2024). Thermal plasma gasification of sewage sludge: optimisation of operating parameters and economic evaluation. *Energy Convers. Manag.* 313: 118639.

Cyranoski, D. (2006). Waste management: one man's trash. *Nature* 444: 262–263.

Dai, L., Zhou, N., Lv, Y., Cheng, Y., Wang, Y., Liu, Y., Cobb, K., Chen, P., Lei, H., and Ruan, R. (2022). Pyrolysis technology for plastic waste recycling: a state-of-the-art review. *Prog. Energy Combust. Sci.* 93: 101021.

Das, S., Hazra, A., and Banerjee, P. (2020). PCDD/PCDFs: a burden from hospital waste disposal plant; plasma arc gasification is the ultimate solution for its mitigation. *Energy Recovery Process Waste*: 9–21.

Demchenko, S., Pihida, Y., and Davydov, S. (2019). Heat exchange processes and productivity of carbon environment transformations of the water-plasma energy stream. *E3S Web Conf.* 109: 00016.

Diab, J., Dames, E., Rohani, V., Wyse, E., and Fulcheri, L. (2024). Review of DC and AC arc plasma at high pressures above atmospheric pressure. *Plasma Chem. Plasma Process.* 44: 687–720.

Dogu, O., Pelucchi, M., Van de Vijver, R., Van Steenberge, P.H.M., D'hooge, D.R., Cuoci, A., Mehl, M., Frassoldati, A., Faravelli, T., and Van Geem, K.M. (2021). The chemistry of chemical recycling of solid plastic waste via pyrolysis and gasification: State-of-the-art, challenges, and future directions. *Prog. Energy Combust. Sci.* 84: 100901.

Domarov, P.V. (2020). Mathematical modeling of plasma-thermal gasification of technogenic wastes. *J. Phys. Conf. Ser.* 1677: 012105.

Dors, M., Nowakowska, H., Jasiński, M., and Mizeraczyk, J. (2014). Chemical kinetics of methane pyrolysis in microwave plasma at atmospheric pressure. *Plasma Chem. Plasma Process.* 34: 313–326.

Ducharme, C. (2010). *Technical and economic analysis of plasma-assisted waste-to-energy processes*. Master's thesis. Columbia University.

Elaissi, S. and Alsaif, N.A.M. (2023). Modeling and performance analysis of municipal solid waste treatment in plasma torch reactor. *Symmetry* 15: 692.

European Environment Agency. (2023). Overview of landfill taxes on municipal waste used in EU member states, Available at: https://www.eea.europa.eu/en/analysis/maps-andcharts/overview-of-landfill-taxes-on (Accessed 7 Jan 2025).

Fathi, J., Hlína, M., Mates, T., Buryi, M., Sikarwar, V.S., Mušálek, R., Sharma, S., Lojka, M., Jiříčková, A., Jankovský, O., et al. (2025). Thermo-chemical recycling of polypropylene via high-power microwave plasma gasification: syngas and metal carbide production. *Chem. Eng. J.* 511: 161910.

Fathi, J., Mašláni, A., Hlína, M., Lukáč, F., Mušálek, R., Jankovský, O., Lojka, M., Jiříčková, A., Skoblia, S., Mates, T., et al. (2024). Multiple benefits of polypropylene plasma gasification to consolidate plastic treatment, CO_2 utilization, and renewable electricity storage. *Fuel* 368: 131692.

Fazekas, P., Czégény, Z., Mink, J., Bódis, E., Klébert, S., Németh, C., Keszler, A.M., Károly, Z., and Szépvölgyi, J. (2016). Decomposition of poly(vinyl chloride) in inductively coupled radiofrequency thermal plasma. *Chem. Eng. J.* 302: 163–171.

Gabbar, H.A., Aboughaly, M., and Stoute, C.A.B. (2017). DC thermal plasma design and utilization for the low density polyethylene to diesel oil pyrolysis reaction. *Energies* 10, https://doi.org/10.3390/en10060784.

Gabbar, H.A., Darda, S.A., Damideh, V., Hassen, I., Aboughaly, M., and Lisi, D. (2021). Comparative study of atmospheric pressure DC, RF, and microwave thermal plasma torches for waste to energy applications. *Sustain. Energy Technol. Assess.* 47: 101447.

Ganza, P.E. and Lee, B. (2023). A novel method for industrial production of clean hydrogen (H_2) from mixed plastic waste. *Int. J. Hydrogen Energy* 48: 15037–15052.

Ghorui, S., Meher, K.C., Kar, R., Tiwari, N., and Sahasrabudhe, S.N. (2016). Unique erosion features of hafnium cathode in atmospheric pressure arcs of air, nitrogen and oxygen. *J. Phys. D Appl. Phys.* 49: 295201.

Ghorui, S., Sahasrabudhe, S.N., and Das, A.K. (2010). Current transfer in DC non-transferred arc plasma torches. *J. Phys. D Appl. Phys.* 43: 245201.

Gollapalli, V., Pathak, R.K., Raghuram, P., Dey, S., Bhaskar, K., Das, A., and Sharma, S. (2024). Use of coke dust as slag de-oxidation agent for improving desulfurization in Si-killed HC steels. *Trans. Indian Inst. Met.* 77: 1859–1871.

Gómez-Barea, A. and Leckner, B. (2010). Modeling of biomass gasification in fluidized bed. *Prog. Energy Combust. Sci.* 36: 444–509.

Gonçalves, M.F.S., Petraconi Filho, G., Couto, A.A., Silva Sobrinho, A.S., Miranda, F.S., and Massi, M. (2022). Evaluation of thermal plasma process for treatment disposal of solid radioactive waste. *J. Environ. Manag.* 311: 114895.

Gracida-Alvarez, U.R., Mitchell, M.K., Sacramento-Rivero, J.C., and Shonnard, D.R. (2018). Effect of temperature and vapor residence time on the micropyrolysis products of waste high-density polyethylene. *Ind. Eng. Chem. Res.* 57: 1912–1923.

Grand View Research. (2024). Plastic to fuel market size & outlook, 2030. Available at: https://www.grandviewresearch.com/horizon/outlook/plastic-to-fuel-market-size/global (Accessed 16 Sep 2024).

Grandesso, E., Ryan, S., Gullett, B., Touati, A., Collina, E., Lasagni, M., and Pitea, D. (2008). Kinetic modeling of polychlorinated dibenzo-p-dioxin and dibenzofuran formation based on carbon degradation reactions. *Environ. Sci. Technol.* 42: 7218–7224.

Green Bank Waste Solutions. (2024). UK landfill tax rates 2024: what you need to know, Available at: https://greenbankwastesolutions.com/landfill-tax-rates-what-you-need-to-know/ (Accessed 7 Jan 2025).

Guddeti, R.R., Knight, R., and Grossmann, E.D. (2000a). Depolymerization of polyethylene using induction coupled plasma technology. *Plasma Chem. Plasma Process.* 20: 37–64.

Guddeti, R.R., Knight, R., and Grossmann, E.D. (2000b). Depolymerization of polypropylene in an induction coupled plasma (ICP) reactor. *Ind. Eng. Chem. Res.* 39: 1171–1176.

Gueye, P., Cressault, Y., Rohani, V., and Fulcheri, L. (2017). A simplified model for the determination of current voltage characteristics of a high-pressure hydrogen plasma arc. *J. Appl. Phys.* 121, https://doi.org/10.1063/1.4976572.

Guo, X.F. and Kim, G.J. (2010). Synthesis of ultrafine carbon black by pyrolysis of polymers using a direct current thermal plasma process. *Plasma Chem. Plasma Process.* 30: 75–90.

Guo, M., Wang, K., Bing, X., Cheng, J., Zhang, Y., Sun, X., Guan, B., and Yu, J. (2024). Pyrolysis of plastics-free refuse derived fuel derived from municipal solid waste and combustion of the char products in lab and pilot scales: a comparative study. *Fuel* 359: 130335.

Hall, S. (2012). *Branan's rules of thumb for chemical engineers*, 5th ed. Elsevier.

Han, S.W., Tokmurzin, D., Lee, J.J., Park, S.J., Ra, H.W., Yoon, S.J., Mun, T.Y., Yoon, S.M., Moon, J.H., Lee, J.G., et al. (2022). Gasification characteristics of waste plastics (SRF) in a bubbling fluidized bed: use of activated carbon and olivine for tar removal and the effect of steam/carbon ratio. *Fuel* 314: 123102.

Hlina, M., Hrabovsky, M., Kavka, T., and Konrad, M. (2014). Production of high-quality syngas from argon/water plasma gasification of biomass and waste. *Waste Manag.* 34: 63–66.

Ho, G.S., Faizal, H.M., and Ani, F.N. (2017). Microwave induced plasma for solid fuels and waste processing: a review on affecting factors and performance criteria. *Waste Manag.* 69: 423–430.

Horton, S.R., Zhang, Y., Mohr, R., Petrocelli, F., and Klein, M.T. (2016). Implementation of a molecular-level kinetic model for plasma-arc municipal solid waste gasification. *Energy Fuels* 30: 7904–7915.

Hrabovsky, M., Jeremias, M., and van Oost, G. (2022). *Plasma gasification and pyrolysis*, 1st ed. Taylor and Francis.

Hrabovsky, M., Konrad, M., Hlina, M., Kopecky, V., Kavka, T., Chumak, O., Maslani, A., Van Oos, G. (2010). *International symposium on non-thermal/thermal plasma pollution control technology & sustainable energy, June 21-25, 2010*, St. John's, Newfoundland, Canada.

Hrabovsky, M. and van der Walt, I.J. (2018). Plasma waste destruction. In: Fracis, A.K. (Ed.). *Handbook of thermal science and engineering*, 1st ed. Springer, International, pp. 2829–2884.

Hu, L., Yu, H., Yan, X., Sun, Y., and Zhu, B. (2023). Analysis of molten slag from high-temperature plasma treatment of oil-based drill cuttings. *Process Saf. Environ. Prot*. 172: 97–104.

Huang, X., Cheng, D.G., Chen, F., and Zhan, X. (2013). A density functional theory study on pyrolysis mechanism of lignin in hydrogen plasma. *Ind. Eng. Chem. Res.* 52: 14107–14115.

Ibrahimoglu, B., Cucen, A., and Yilmazoglu, M.Z. (2017). Numerical modeling of a downdraft plasma gasification reactor. *Int. J. Hydrogen Energy* 42: 2583–2591.

Inayat, A., Tariq, R., Khan, Z., Ghenai, C., Kamil, M., Jamil, F., and Shanableh, A. (2023). A comprehensive review on advanced thermochemical processes for bio-hydrogen production via microwave and plasma technologies. *Biomass Convers. Biorefin.* 13: 8593–8602.

Ismail, T.M., Ramos, A., Abd El-Salam, M., Monteiro, E., and Rouboa, A. (2019). Plasma fixed bed gasification using an Eulerian model. *Int. J. Hydrogen Energy* 44: 28668–28684.

Janajreh, I., Raza, S.S., and Valmundsson, A.S. (2013). Plasma gasification process: modeling, simulation and comparison with conventional air gasification. *Energy Convers. Manag.* 65: 801–809.

Janajreh, I., Adeyemi, I., Raza, S.S., and Ghenai, C. (2021). A review of recent developments and future prospects in gasification systems and their modeling. *Renew. Sustain. Energy Rev.* 138, https://doi.org/10.1016/j.rser.2020.110505.

Jiang, Y., Leng, B., and Xi, J. (2024). Assessing the social cost of municipal solid waste management in Beijing: a systematic life cycle analysis. *Waste Manag.* 173: 62–74.

Jones, W.P. and Lindstedt, R.P. (1988). Global reaction schemes for hydrocarbon combustion. *Combust. Flame* 73: 233–249.

Joseph, B., James, J., Kalarikkal, N., and Thomas, S. (2021). Recycling of medical plastics. *Adv. Ind. Eng. Polym. Res.* 4: 199–208.

Joshi, J.B. (2001). Computational flow modelling and design of bubble column reactors. *Chem. Eng. Sci.* 56: 5893–5933.

Kaushal, R., Rohit, and Dhaka, A.K. (2024). A comprehensive review of the application of plasma gasification technology in circumventing the medical waste in a post-COVID-19 scenario. *Biomass Convers. Biorefin.* 14: 1427–1442.

Kholiavchenko, L., Pihida, Y., Demchenko, S., and Davydov, S. (2019). Determination of the kinetic constants of the process of plasma gasification of coal-water fuel. *E3S Web Conf.* 109: 00034.

Kibria, M.G., Masuk, N.I., Safayet, R., Nguyen, H.Q., and Mourshed, M. (2023). Plastic waste: challenges and opportunities to mitigate pollution and effective management. *Int. J. Environ. Res.* 17: 1–37.

Kwon, S. and Im, S. (2024). Thermodynamic evaluation of integrated plasma gasification combined cycle with plastic waste feedstock. *Chem. Eng. J.* 482: 148771.

Lázár, M., Hnatko, M., Sedláček, J., Čarnogurská, M., and Brestovič, T. (2018). Upgrading the glassy slag from waste disposal by thermal plasma treatment. *Waste Manag.* 78: 173–182.

Lee, M.K.K. (2021). Plastic pollution mitigation – net plastic circularity through a standardized credit system in Asia. *Ocean Coast. Manag.* 210: 105733.

Levenspiel, O. (1999). Chemical reaction engineering. *Ind. Eng. Chem. Res.* 38: 4140–4143.

Li, S., Chen, H., Gao, Y., Fan, L., Pan, P., and Xu, G. (2024). A novel waste-to-energy system based on sludge hydrothermal treatment and medical waste plasma gasification and integrated with the waste heat recovery of a cement plant. *Energy* 305: 132358.

Li, Y.J., Pei, S.L., Sun, Z.H., Zhong, L., He, C.C., Pan, S.Y., Li, Y.J., Pei, S.L., Kim, K.H., Rinklebe, O., et al. (2023). Comprehensive performance evaluation of plasma vitrification for detoxification and valorization of residual wastes. *Crit. Rev. Environ. Sci. Technol.* 53: 527–549.

Liavonchyk, A., Dalholenka, H., Skavysh, U., and Sauchyn, V. (2021). Effect of accounting radiation heat transfer in numerical modeling of partial oxidation of hydrocarbons in a plasma reactor. *High Temp. Mater. Process.* 25: 15–23.

Liavonchyk, A., Morozov, D., Sauchyn, V., and Dalholenka, H. (2017). Numerical modeling of processes in a plasma reactor for conversion of hydrocarbons. *High Temp. Mater. Process.* 21: 359–375.

Lopez, G., Artetxe, M., Amutio, M., Alvarez, J., Bilbao, J., and Olazar, M. (2018). Recent advances in the gasification of waste plastics. A critical overview. *Renew. Sustain. Energy Rev.* 82: 576–596.

Montiel-Bohórquez, N.D., Agudelo, A.F., and Pérez, J.F. (2022). Modelling of an integrated plasma gasification combined cycle power plant using Aspen Plus. *J. King Saud Univ. Eng. Sci.* 36: 620–631.

Ma, W.C., Chu, C., Wang, P., Guo, Z.F., Lei, S.J., Zhong, L., and Chen, G.Y. (2020). Hydrogen-rich syngas production by DC thermal plasma steam gasification from biomass and plastic mixtures. *Adv. Sustain. Syst.* 4: 2000026.

Ma, W., Chu, C., Wang, P., Guo, Z., Liu, B., and Chen, G. (2020). Characterization of tar evolution during DC thermal plasma steam gasification from biomass and plastic mixtures: parametric optimization via response surface methodology. *Energy Convers. Manag.* 225: 113407.

Ma, Y., Chu, H., and Zheng, B. (2024). Research progress of plasma melting technology in radioactive waste treatment of nuclear power plants. *Ann. Nucl. Energy* 198: 110307.

Ma, M., Qi, C., Lin, X., Zhao, R., Wang, Z., Wang, G., Liu, M., Zhu, Z., and Niu, C. (2023). Composition modification and plasma vitrification of bottom ash from industrial hazardous waste incineration. *J. Non-Cryst. Solids* 619: 122579.

Ma, W., Shi, W., Shi, Y., Chen, D., Liu, B., Chu, C., Li, D., Li, Y., and Chen, G. (2021). Plasma vitrification and heavy metals solidification of MSW and sewage sludge incineration fly ash. *J. Hazard. Mater.* 408: 124809.

Ma, J., Su, B., Wen, G., Ren, Q., Yang, Y., Yang, Q., and Xing, H. (2016). Kinetic modeling and experimental validation of the pyrolysis of propane in hydrogen plasma. *Int. J. Hydrogen Energy* 41: 22689 22697.

MacLeod, M., Arp, H.P.H., Tekman, M.B., and Jahnke, A. (2021). The global threat from plastic pollution. *Science* 373: 61–65.

Mączka, T., Śliwka, E., and Wnukowski, M. (2013). Plasma gasification of waste plastics. *J. Ecol. Eng.* 14: 33–39.

Mahinpey, N. and Gomez, A. (2016). Review of gasification fundamentals and new findings: reactors, feedstock, and kinetic studies. *Chem. Eng. Sci.* 148: 14–31.

Martínez-Narro, G., Royston, N.J., Billsborough, K.L., and Phan, A.N. (2023). Kinetic modelling of mixed plastic waste pyrolysis. *Chem. Thermodyn. Therm. Anal.* 9: 100105.

Massman, W.J. (1998). A review of the molecular diffusivities of H_2O, CO_2, CH_4, CO, O_3, SO_2, NH_3, N_2O, NO, and NO_2 in air, O_2 and N_2 near STP. *Atmos. Environ.* 32: 1111–1127.

Mastellone, M.L., Zaccariello, L., and Arena, U. (2010). Co-gasification of coal, plastic waste and wood in a bubbling fluidized bed reactor. *Fuel* 89: 2991–3000.

Mazzoni, L. (2017). *Techno-economic analysis of energy recovery from municipal and industrial waste through plasma gasification*, Master's thesis. Khalifa University.

Mazzoni, L. and Janajreh, I. (2017). Plasma gasification of municipal solid waste with variable content of plastic solid waste for enhanced energy recovery. *Int. J. Hydrogen Energy* 42: 19446–19457.

Midilli, A., Kucuk, H., Haciosmanoglu, M., Akbulut, U., and Dincer, I. (2022). A review on converting plastic wastes into clean hydrogen via gasification for better sustainability. *Int. J. Energy Res*. 46, https://doi.org/10.1002/er.7498.

Mohsenian, S., Esmaeili, M.S., Fathi, J., and Shokri, B. (2018). Synthesis of carbon nano-spheres and nano-tubes by thermal plasma processing of polypropylene. *Appl. Phys. A* 124: 1–6.

Mohsenian, S., Esmaili, M.S., Fathi, J., and Shokri, B. (2016). Hydrogen and carbon black nano-spheres production via thermal plasma pyrolysis of polymers. *Int. J. Hydrogen Energy* 41: 16656–16663.

Mtibe, A., Mokhena, T.C., and John, M.J. (2023). Sustainable valorization and conversion of e-waste plastics into value-added products. *Curr. Opin. Green Sustain. Chem.* 40: 100762.

Mukherjee, C., Denney, J., Mbonimpa, E.G., Slagley, J., and Bhowmik, R. (2020). A review on municipal solid waste-to-energy trends in the USA. *Renew. Sustain. Energy Rev.* 119: 109512.

Mukherjee, A., Ruj, B., Sadhukhan, A.K., Gupta, P., Parashar, C.K., and Chatterjee, P.K. (2024). Applications of H2 enriched syngas and slag products from plastic wastes via novel plasma dual-stage-arc pyrolysis. *J. Environ. Manag.* 370: 123025.

Munir, M.T., Mardon, I., Al-Zuhair, S., Shawabkeh, A., and Saqib, N.U. (2019). Plasma gasification of municipal solid waste for waste-to-value processing. *Renew. Sustain. Energy Rev.* 116: 109461.

Munz, R.J. and Habelrih, M. (1992). Cathode erosion on copper electrodes in steam, hydrogen, and oxygen plasmas. *Plasma Chem. Plasma Process.* 12: 203–218.

Nagar, V. and Kaushal, R. (2024). A review of recent advancement in plasma gasification: a promising solution for waste management and energy production. *Int. J. Hydrogen Energy* 77: 405–419.

Nemmour, A., Inayat, A., Janajreh, I., and Ghenai, C. (2023). Syngas production from municipal solid waste plasma gasification: a simulation and optimization study. *Fuel* 349: 128698.

Obraztsov, N.V., Safronov, A.A., Subbotin, D.I., Ivanov, D., and Dudnik, J.D. (2019). The usage of low-voltage AC plasma torch for polystyrene gasification. In: *IOP Conf. Ser. Mater. Sci. Eng. May 23-24, 2019*, Saint Petersburg, Russian Federation.

Ofori-Boateng, C. (2024). Exergy and life cycle analyses of thermochemical waste conversion technologies. In: Ofori-Boateng, C. (Ed.). *Sustainability of thermochemical waste conversion technologies*. 1st ed. Springer, Cham, pp. 129–159.

Okati, A., Khani, M.R., Shokri, B., Monteiro, E., and Rouboa, A. (2021). Numerical modeling of plasma gasification process of polychlorinated biphenyl wastes. *Energy Rep.* 7: 270–285.

Oliveira, M., Ramos, A., Ismail, T.M., Monteiro, E., and Rouboa, A. (2022). A review on plasma gasification of solid residues: recent advances and developments. *Energies* 15: 1475.

Our World in Data. (2024). *How much of global greenhouse gas emissions come from plastics?* Available at: https://ourworldindata.org/ghg-emissions-plastics (Accessed 16 Sep 2024).

Pancholi, K.C., Sen, N., Singh, K.K., Vincent, T., and Kaushik, C.P. (2022). Transient heat transfer during startup of a thermal plasma chamber: numerical insights. *Prog. Nucl. Energy* 152: 104371.

Park, H.S., Kim, C.G., and Kim, S.J. (2006). Characteristics of PE gasification by steam plasma. *J. Ind. Eng. Chem.* 12: 216–223.

Park, J.H., Park, H.W., Choi, S., and Park, D.W. (2016). Effects of blend ratio between high density polyethylene and biomass on co-gasification behavior in a two-stage gasification system. *Int. J. Hydrogen Energy* 41: 16813–16822.

Paulino, R.F.S., Essiptchouk, A.M., Costa, L.P.C., and Silveira, J.L. (2022). Thermodynamic analysis of biomedical waste plasma gasification. *Energy* 244: 122600.

Paulino, R.F.S., Essiptchouk, A.M., and Silveira, J.L. (2020). The use of syngas from biomedical waste plasma gasification systems for electricity production in internal combustion: thermodynamic and economic issues. *Energy* 199: 117419.

Perez, B.A., Jayarama Krishna, J.V., and Toraman, H.E. (2023). Insights into co-pyrolysis of polyethylene terephthalate and polyamide 6 mixture through experiments, kinetic modeling and machine learning. *Chem. Eng. J.* 468: 143637.

Peters, B., Džiugys, A., and Navakas, R. (2012). A shrinking model for combustion/gasification of char based on transport and reaction time scales. *Mechanika* 18, https://doi.org/10.5755/j01.mech.18.2.1564.

Pitrez, P., Monteiro, E., and Rouboa, A. (2023). Numerical analysis of plasma gasification of hazardous waste using Aspen Plus. *Energy Rep.* 9: 418–426.

Pulse. (2024). World's first microwave-driven plasma gasification plant plugs in Korea in April - 매일경제 영문뉴스 펄스 (Pulse), Available at: https://pulse.mk.co.kr/news/english/9706156 (Accessed 16 Sep 2024).

Punčochář, M., Ruj, B., and Chatterjee, P.K. (2012). Development of process for disposal of plastic waste using plasma pyrolysis technology and option for energy recovery. *Procedia Eng.* 42: 420–430.

Qing, N.K.C., Samiran, N.A., and Rashid, R.A. (2022). CFD simulation analysis of sub-component in municipal solid waste gasification using plasma downdraft technique. *CFD Lett.* 14: 63–70.

Qureshi, M.S., Oasmaa, A., Pihkola, H., Deviatkin, I., Tenhunen, A., Mannila, J., Minkkinen, H., Pohjakallio, M., and Laine-Ylijoki, J. (2020). Pyrolysis of plastic waste: opportunities and challenges. *J. Anal. Appl. Pyrolysis* 152: 104804.

Rabou, L.P.L.M., Zwart, R.W.R., Vreugdenhil, B.J., and Bos, L. (2009). Tar in biomass producer gas, the Energy Research Centre of the Netherlands (ECN) experience: an enduring challenge. *Energy Fuels* 23: 6189–6198.

Ramos, A., Monteiro, E., and Rouboa, A. (2019a). Numerical approaches and comprehensive models for gasification process: a review. *Renew. Sustain. Energy Rev.* 110: 188–206.

Ramos, A. and Rouboa, A. (2022). Life cycle thinking of plasma gasification as a waste-to-energy tool: review on environmental, economic and social aspects. *Renew. Sustain. Energy Rev.* 153: 111762.

Ramos, A., Teixeira, C.A., and Rouboa, A. (2019b). Environmental assessment of municipal solid waste by two stage plasma gasification. *Energies* 12: 137.

Razak, S.M., Sharma, K., Nair, T., Munagala, C.K., and Aniya, V. (2024). Hydrogen production potential from plastic pyrolysis oil: experimental and economic insights. *J. Environ. Chem. Eng.* 12: 112220.

Rida Galaly, A., Van Oost, G., and Dawood, N. (2024). Sustainable plasma gasification treatment of plastic waste: evaluating environmental, economic, and strategic dimensions. *ACS Omega* 9: 21174 21186.

Rojas-Perez, F., Castillo-Benavides, J.A., Richmond-Navarro, G., and Zamora, E. (2018). CFD modeling of plasma gasification reactor for municipal solid waste. *IEEE Trans. Plasma Sci.* 46: 2435–2444.

Rutberg, P.G., Kuznetsov, V.A., Serba, E.O., Popov, S.D., Surov, A.V., Nakonechny, G.V., and Nikonov, A.V. (2013). Novel three-phase steam-air plasma torch for gasification of high-caloric waste. *Appl. Energy* 108: 505–514.

Safavi, S.M., Richter, C., Safavi, A., and Unnthorsson, R. (2021). Dioxin and furan emissions from gasification. In: Silva, V., and Tuna, C. (Eds.). *Gasification*. InTech.

Safavi, A., Richter, C., and Unnthorsson, R. (2022). Dioxin formation in biomass gasification: a review. *Energies* 15: 700.

Sakhraji, M., Ramos, A., Monteiro, E., Bouziane, K., and Rouboa, A. (2022). Plasma gasification process using computational fluid dynamics modeling. *Energy Rep.* 8: 1541–1549.

Sampathraju, R. and Mansuri, A. (2019). Assessment of air pollutants in the occupational environment of plasma biomedical waste disposal system in Ahmedabad, India. *J. Environ. Saf.* 10: 89–93.

Sanito, R.C., Bernuy-Zumaeta, M., You, S.J., and Wang, Y.F. (2022). A review on vitrification technologies of hazardous waste. *J. Environ. Manag.* 316: 115243.

Sanlisoy, A. and Ozdinc Carpinlioglu, M. (2019). Microwave plasma gasification of a variety of fuel for syngas production. *Plasma Chem. Plasma Process.* 39: 1211–1225.

Sedej, O. and Mbonimpa, E. (2021). CFD modeling of a lab-scale microwave plasma reactor for waste-to energy applications: a review. *Gases* 1: 133–147.

Sekiguchi, H. and Orimo, T. (2004). Gasification of polyethylene using steam plasma generated by microwave discharge. *Thin Solid Films* 457: 44–47.

Sesotyo, P.A., Nur, M., and Suseno, J.E. (2019). Plasma gasification with municipal solid waste as a method of energy self-sustained for better urban built environment: modeling and simulation. *IOP Conf. Ser. Earth Environ. Sci.* 396: 012002.

SGH2 Energy. (2024). Available at: https://www.sgh2energy.com/ (Accessed 16 Sep 2024).

Shah, H.H., Amin, M., Iqbal, A., Nadeem, I., Kalin, M., Soomar, A.M., and Galal, A.M. (2023). A review on gasification and pyrolysis of waste plastics. *Front. Chem.* 10: 960894.

Sharma, A.K. (2008). Equilibrium modeling of global reduction reactions for a downdraft (biomass) gasifier. *Energy Convers. Manag.* 49: 832–842.

Sharma, K.L.S. (2017). *Overview of industrial process automation*, 2nd ed. Elsevier Inc.

Shevchenko, V., Oparin, S., and Kabakova, L. (2024). Methodology for determining the design parameters of combined type plasma-chemical reactor for gasification of carbon-containing raw materials. *IOP Conf. Ser. Earth Environ. Sci.* 1348: 012078.

Shi, H., Wang, S., and Wang, P. (2024). From simulation to reality: CFD-ML-driven structural optimization and experimental analysis of thermal plasma reactors. *J. Environ. Chem. Eng.* 12: 112998.

Shuangning, X., Weiming, Y., and Li, B. (2005). Flash pyrolysis of agricultural residues using a plasma heated laminar entrained flow reactor. *Biomass Bioenergy* 29: 135–141.

Sikarwar, V.S., Hrabovský, M., Van Oost, G., Pohořelý, M., and Jeremiáš, M. (2020). Progress in waste utilization via thermal plasma. *Prog. Energy Combust. Sci.* 81: 100873.

Sikarwar, V.S., Masláni, A., Hlína, M., Fathi, J., Mates, T., Pohorelý, M., Meers, E., Šyc, M., and Jeremias, M. (2022a). Thermal plasma assisted pyrolysis and gasification of RDF by utilizing sequestered CO_2 as gasifying agent. *J. CO2 Util.* 66: 102275.

Sikarwar, V.S., Mašláni, A., Van Oost, G., Fathi, J., Hlína, M., Mates, T., Pohořelý, M., and Jeremias, M. (2024). Integration of thermal plasma with CCUS to valorize sewage sludge. *Energy* 288: 129896.

Sikarwar, V.S., Peela, N.R., Vuppaladadiyam, A.K., Ferreira, N.L., Mašláni, A., Tomar, R., Pohořelý, M., Meers, E., and Jeremiáš, M. (2022b). Thermal plasma gasification of organic waste stream coupled with CO_2-sorption enhanced reforming employing different sorbents for enhanced hydrogen production. *RSC Adv.* 12: 6122–6132.

Sikarwar, V.S., Reichert, A., Pohorely, M., Meers, E., Ferreira, N.L., and Jeremias, M. (2021). Equilibrium modeling of thermal plasma assisted co-valorization of difficult waste streams for syngas production. *Sustain. Energy Fuels* 5: 4650–4660.

Singhal, A., Gupta, A.K., Dubey, B., and Ghangrekar, M.M. (2022). Seasonal characterization of municipal solid waste for selecting feasible waste treatment technology for Guwahati city, India. *J. Air Waste Manag. Assoc.* 72: 147–160.

Sniadecka, N., Tonderski, A., Hanel, A., Wojda-Gburek, J., and Hupka, J. (2016). Mineral matter in municipal solid waste. *Physicochem. Probl. Miner. Process.* 52.

Stankiewicz, A. (2020). The principles and domains of process intensification. *Chem. Eng. Prog.* 116: 23–28.

Statista. (2025). U.S. landfill dump fees by region 2023. Available at: https://www.statista.com/statistics/692063/cost-to-landfill-municipal-solid-waste-by-us-region/ (Accessed 6 Jan 2025).

Subbotin, D.I., Surov, A.V., Kuznetsov, V.E., Popov, V.E., Dudnik, J.D., Kuchina, J.D., and Obraztsov, N.V. (2018). Erosion of rod electrodes of the air AC plasma torch. *J. Phys. Conf. Ser.* 1038: 012131.

Surov, A.V., Popov, S.D., Popov, V.E., Subbotin, D.I., Serba, E.O., Spodobin, V.A., Nakonechny, G.V., and Pavlov, A.V. (2017). Multi-gas AC plasma torches for gasification of organic substances. *Fuel* 203: 1007–1014.

Syarif, T., Sulistyo, H., Sediawan, W.B., Anshakov, A.S., Domarov, P.V., and Faleev, V.A. (2019). Simulation of heat and mass transfer in a shaft plasma furnace for the processing of municipal solid waste. *J. Phys. Conf. Ser.* 1382: 012130.

Szente, R.N., Munz, R.J., and Drouet, M.G. (1992). Electrode erosion in plasma torches. *Plasma Chem. Plasma Process.* 12: 327–343.

Tang, L. and Huang, H. (2007). Decomposition of polyethylene in radio-frequency nitrogen and water steam plasmas under reduced pressures. *Fuel Process. Technol*. 88: 549–556.

Tang, L., Huang, H., Hao, H., and Zhao, K. (2013). Development of plasma pyrolysis/gasification systems for energy efficient and environmentally sound waste disposal. *J. Electrostat.* 71: 839–847.

Tang, L., Huang, H., Zhao, Z., Wu, C.Z., and Chen, Y. (2003). Pyrolysis of polypropylene in a nitrogen plasma reactor. *Ind. Eng. Chem. Res.* 42: 1145–1150.

Tang, Y., Tao, D., Li, G., Ye, C., Bu, Z., Shen, R., Lin, Y., and Lv, W. (2024). Formation behavior of PCDD/Fs during waste pyrolysis and incineration: effect of temperature, calcium oxide addition, and redox atmosphere. *Environ. Pollut.* 350: 124011.

Tavares, R., Ramos, A., and Rouboa, A. (2019). A theoretical study on municipal solid waste plasma gasification. *Waste Manag.* 90: 37–45.

Tessier, A., Campbell, P.G.C., and Bisson, M. (1979). Sequential extraction procedure for the speciation of particulate trace metals. *Anal. Chem.* 51: 844–851.

Thynell, S.T. (1998). Discrete-ordinates method in radiative heat transfer. *Int. J. Eng. Sci.* 36: 1651–1675.

Tonks, L. and Langmuir, I. (1929). Oscillations in ionized gases. *Phys. Rev.* 33: 195.

Tu, W.K., Shie, J.L., Chang, C.Y., Chang, C.F., Lin, C.F., Yang, S.Y., Kuo, J.T., Shaw, D.G., You, Y.D., and Lee, D.J. (2009). Products and bioenergy from the pyrolysis of rice straw via radio frequency plasma and its kinetics. *Bioresour. Technol.* 100: 2052–2061.

UNEP. (2024). *Legal limits on single-use plastics and microplastics: a global review of national laws and regulations*. UNEP – UN Environment Programme. Available at: https://www.unep.org/resources/publication/legal-limits-single-use-plastics-and-microplasticsglobal-review-national (Accessed 16 Sep 2024).

Venkatramani, N. (2002). Industrial plasma torches and applications. *JSTOR* 83: 254–262.

Vox, G., Loisi, R.V., Blanco, I., Mugnozza, G.S., and Schettini, E. (2016). Mapping of agriculture plastic waste. *Agric. Agric. Sci. Procedia.* 8: 583–591.

Wang, S., Shi, H., and Wang, P. (2025). Techno-economic and scalability analysis of nitrogen plasma gasification of medical waste. *Waste Manag* 198: 55–65.

Westbrook, C.K. and Dryer, F.L. (1981). Simplified reaction mechanisms for the oxidation of hydrocarbon fuels in flames. *Combust. Sci. Technol.* 27: 31–43.

Wilk, V. and Hofbauer, H. (2013). Conversion of mixed plastic wastes in a dual fluidized bed steam gasifier. *Fuel* 107: 787–799.

Yadav, M.D., Dasgupta, K., Patwardhan, A.W., and Joshi, J.B. (2017). High performance fibers from carbon nanotubes: synthesis, characterization and applications in composites – a review. *Ind. Eng. Chem. Res.* 56: 12407.

Yepes Maya, D.M., Espinosa Sarmiento, A.L., Vilas Boas de Sales Oliveira, C.A., Silva Lora, E.E., and Vieira Andrade, R. (2016). Gasification of municipal solid waste for power generation in Brazil, a review of available technologies and their environmental benefits. *J. Chem. Chem. Eng.* 10, https://doi.org/10.17265/1934-7375/2016.06.001.

Yousef, S., Tamošiūnas, A., Aikas, M., Uscila, R., Gimžauskaitė, D., and Zakarauskas, K. (2024). Plasma steam gasification of surgical mask waste for hydrogen-rich syngas production. *Int. J. Hydrogen Energy* 49: 1375–1386.

Yun, Y.M., Seo, M.W., Ra, H.W., Yoon, S.J., Mun, T.Y., Moon, J.H., Kook, J.W., Kim, Y.K., Lee, J.G., and Kim, J.H. (2017). Gasification characteristics of glass fiber-reinforced plastic (GFRP) wastes in a microwave plasma reactor. *Korean J. Chem. Eng.* 34: 2756–2763.

Zairin, D.M., Ruiz, M.P., and Kersten, S.R.A. (2024). Pyrolysis of polyethylene: chemical kinetics, mass transfer, and reflux system. *Energy Fuels* 39: 1015–1025.

Zamri, A.A., Ong, M.Y., Nomanbhay, S., and Show, P.L. (2021). Microwave plasma technology for sustainable energy production and the electromagnetic interaction within the plasma system: a review. *Environ. Res.* 197: 111204.

Zhang, M., Ma, J., Su, B., Wen, G., Yang, Q., and Ren, Q. (2017). Pyrolysis of polyolefins using rotating arc plasma technology for production of acetylene. *Energies* 10: 513.

Zhang, Q., Dor, L., Biswas, A.K., Yang, W., and Blasiak, W. (2013). Modeling of steam plasma gasification for municipal solid waste. *Fuel Process. Technol.* 106: 546–554.

Zhang, Y., Fu, Z., Wang, W., Ji, G., Zhao, M., and Li, A. (2022). Kinetics, product evolution, and mechanism for the pyrolysis of typical plastic waste. *ACS Sustain. Chem. Eng.* 10: 91–103.

Zhang, R.-Z., Luo, Y.-H., and Yin, R.-H. (2018). Experimental study on dioxin formation in an MSW gasification-combustion process: an attempt for the simultaneous control of dioxins and nitrogen oxides. *Waste Manag.* 82: 292–301.

Zhang, M., Ma, J., Wen, G., Yang, Q., Su, B., and Ren, Q. (2018). Gas production from polyethylene terephthalate using rotating arc plasma. *Chem. Eng. Process. – Process Intensif.* 128: 257–262.

Zhang, F., Tavakkol, S., Galeazzo, F.C.C., and Stapf, D. (2024). Particle-resolved simulation of the pyrolysis process of a single plastic particle. *Heat Mass Transfer* 61: 12.

Zhang, C., Wang, F., Shi, Y., Li, J., and Wu, Y. (2024). Numerical simulation of performance characteristics and structure optimization of plasma gasifier based on hydrodynamics. *Combust. Sci. Technol.* 196: 4469–4486.

Zhao, Z., Mo, W., Zhao, G., Zhang, Y., Guo, H., Feng, J., Yang, Z., Wei, D., Fan, X., and Wei, X.Y. (2024). Composition and structural characteristics of coal gasification slag from Jinhua furnace and its thermochemical conversion performance. *Sustainability* 16: 5824.

Zhovtyansky, V. and Valinčius, V. (2018). Chapter 9. Efficiency of plasma gasification technologies for hazardous waste treatment. In: *Gasification for low-grade feedstock*. InTech.

Supplementary Material: This article contains supplementary material (https://doi.org/10.1515/revce-2025-0012).